Analysis of Compatible Discrete Operator Schemes for the Stokes Equations on Polyhedral Meshes

Jérôme Bonelle, Alexandre Ern

Analysis of Compatible Discrete Operator Schemes for the Stokes Equations on Polyhedral Meshes

Jerome Bonelle
EDF R&D
6, quai Watier, BP 49
78401 Chatou cedex
jerome.bonelle@edf.fr

Alexandre Ern
Université Paris-Est, CERMICS
Ecole des Ponts ParisTech
77455 Marne la Vallée Cedex 2, France
ern@cermics.enpc.fr

January 30, 2014

Abstract

Compatible Discrete Operator schemes preserve basic properties of the continuous model at the discrete level. They combine discrete differential operators that discretize exactly topological laws and discrete Hodge operators that approximate constitutive relations. We devise and analyze two families of such schemes for the Stokes equations in curl formulation, with the pressure degrees of freedom located at either mesh vertices or cells. The schemes ensure local mass and momentum conservation. We prove discrete stability by establishing novel discrete Poincaré inequalities. Using commutators related to the consistency error, we derive error estimates with first-order convergence rates for smooth solutions. We analyze two strategies for discretizing the external load, so as to deliver tight error estimates when the external load has a large irrotational or divergence-free part. Finally, numerical results are presented on three-dimensional polyhedral meshes.

1 Introduction

Compatible Discrete Operator (CDO) schemes belong to the broad class of compatible or mimetic schemes, which preserve basic properties of the continuous model at the discrete level; see [3, 4, 8, 12, 14, 16, 20, 28, 33, 36, 40, 42] and references therein. Following the seminal ideas of [41] and [10], the degrees of freedom (DoFs) are defined using de Rham maps, and their localization results from the physical nature of the fields. Moreover, a distinction is operated between topological laws (that are discretized exactly) and constitutive relations (that are approximated). CDO schemes are formulated using discrete differential operators for the topological laws and discrete Hodge operators for the constitutive relations. The discrete differential operators produce a cochain complex, they commute with the de Rham maps, and discrete adjunction properties hold between these operators. The discrete Hodge operator is the key operator in the CDO framework. The design of this operator is not unique, and each design leads to a specific scheme [see 39, 29, 9]. CDO schemes involve two meshes: a primal mesh (which is the only one seen by the end-user) and a dual mesh. The discrete Hodge operator links DoFs defined on the primal mesh to DoFs defined on the dual mesh. In [9], CDO schemes have been analyzed for elliptic problems on polyhedral meshes.

The Stokes equations model flows of incompressible and viscous fluids where the advective inertial forces are negligible with respect to the viscous forces. In this paper, we focus on the stationary Stokes equations posed on an open, bounded and connected domain $\Omega \subset \mathbb{R}^3$ with boundary $\partial\Omega$ and outward normal $\underline{\nu}_{\partial\Omega}$. Our starting point is to formulate the viscous stresses in the momentum balance using the curl operator. This way, all the terms in the Stokes equations can be interpreted using scalar-valued differential forms. We analyze two formulations. The first one, hereafter called 2-field curl formulation,

takes the form

$$\begin{cases} \underline{\mathrm{curl}}(\underline{\mathrm{curl}}(\underline{u})) + \underline{\mathrm{grad}}(p) &= \underline{f}, \qquad \text{in } \Omega, \\ \mathrm{div}(\underline{u}) &= 0, \qquad \text{in } \Omega, \end{cases} \tag{1}$$

where p is the pressure, $\underline{u}$ the velocity and $\underline{f}$ the external load. Introducing the vorticity $\underline{\omega} := \underline{\mathrm{curl}}\,\underline{u}$, the second formulation, hereafter called 3-field curl formulation (also called Velocity-Vorticity-Pressure formulation in the literature), takes the form

$$\begin{cases} -\underline{\omega} + \underline{\mathrm{curl}}(\underline{u}) &= \underline{0}, \qquad \text{in } \Omega, \\ \underline{\mathrm{curl}}(\underline{\omega}) + \underline{\mathrm{grad}}(p) &= \underline{f}, \qquad \text{in } \Omega, \\ \mathrm{div}(\underline{u}) &= 0, \qquad \text{in } \Omega. \end{cases} \tag{2}$$

Essential and natural boundary conditions (BCs) can be considered for both formulations. The first set of BCs enforces the value of the normal component of the velocity $\underline{u} \cdot \underline{\nu}_{\partial\Omega}$ and that of the tangential components of the vorticity $\underline{\omega} \times \underline{\nu}_{\partial\Omega}$ at the boundary. These BCs are natural for (1) and essential for (2). As the pressure is then determined up to an additive constant, the additional requirement of p having zero mean-value is typically added. The second set of BCs enforces the value of the tangential components of the velocity $\underline{u} \times \underline{\nu}_{\partial\Omega}$ and the value of the pressure at the boundary. These BCs are essential for (1) and natural for (2).

Mimetic or compatible schemes for the Stokes equations using either the 2-field or the 3-field curl formulation with the above BCs have already been investigated. Most of the work dedicated to the Stokes equations in curl formulations addresses the 3-field curl formulation (2). Based on the seminal work of [35], [23, 24] first analyzed this formulation in the context of finite elements (FE), and [7] in the context of spectral discretization. More recently, [30] proposed a scheme based on the Mimetic Spectral Element method in 2D and 3D for general quadrilateral/hexahedral meshes, and [19] designed a Discrete Duality Finite Volume (DDFV) scheme for general 2D meshes. Concerning the 2-field curl formulation, only the papers of [11] and of [1] have addressed this formulation on simplicial meshes; see also [37] and [25] for staggered schemes on triangular Delaunay meshes.

In the present work, we devise and analyze CDO schemes for the Stokes problem in both 2-field and 3-field curl formulations. The CDO schemes involve two Hodge operators, one linking the velocity (seen as a circulation) to the mass flux and the other linking the vorticity to the viscous stress. One key feature of the present schemes is that they ensure local mass and momentum conservation on polyhedral meshes. We prove discrete stability by establishing novel discrete Poincaré inequalities in the CDO framework. The present schemes do not need any stabilization. Moreover, using commutators related to the consistency error as in [10, 29, 9], we derive *a priori* error estimates and establish first-order error estimates for smooth solutions. In addition, we show how the present CDO framework can deal with the practically important issue of discretizing the external load, so as to deliver tight error estimates when the external load is expected to have a large irrotational or divergence-free part (see [32] for a related work).

The more classical formulation of the Stokes equations uses the vector Laplacian of the velocity in the momentum balance. Various schemes were proposed to discretize this formulation on polygonal or polyhedral meshes, including Mixed Finite Volumes by [22], Mimetic Finite Differences (MFD) by [5, 6], DDFV by [31], and an extension of the Crouzeix–Raviart finite element by [21]. [27] investigated a scheme for triangular meshes within the Finite Element Exterior Calculus (FEEC) framework. Discretizing the vector Laplacian with CDO schemes is the subject of ongoing work.

This paper is organized as follows. In Section 2, we briefly recall the CDO framework. Then, we investigate CDO schemes for the Stokes equations in the curl formulations (1) and (2). Since the pressure is seen as a potential, its DoFs are located at primal or dual mesh vertices. The former case, treated in Section 3, hinges on the 2-field curl formulation (1) leading to vertex-based pressure schemes. The latter case, treated in Section 4, hinges on the 3-field curl formulation (2) leading to cell-based pressure schemes (since primal cells are in one-to-one correspondence with dual mesh vertices). The vertex-based pressure schemes are, to our knowledge, the first of this class on polyhedral meshes. The cell-based pressure schemes share common features with the recent Mimetic Spectral Element schemes of [30];

the present schemes can be deployed on polyhedral meshes and offer two strategies for discretizing the external load. Finally, we present numerical results in Section 5. For simplicity, we often assume in what follows that Ω is simply connected and that its boundary $\partial\Omega$ is connected. Whenever needed, we refer to this assumption as ($\mathbf{H_\Omega}$).

2 The CDO Framework

2.1 Meshes and degrees of freedom

The discretization of the domain $\Omega \subset \mathbb{R}^3$ relies on a primal mesh $\mathrm{M} = \{\mathrm{V}, \mathrm{E}, \mathrm{F}, \mathrm{C}\}$, where V collects primal vertices (or 0-cells) generically denoted v, E primal edges (or 1-cells) e, F primal faces (or 2-cells) f, and C primal cells (or 3-cells) c. The primal mesh has the structure of a cell complex: the boundary of a k-cell in M, $1 \le k \le 3$, can be decomposed into $(k-1)$-cells belonging to M. The spaces of DoFs are denoted $\mathcal{V}, \mathcal{E}, \mathcal{F}, \mathcal{C}$ and are defined as the codomains of de Rham maps acting as follows:

$$\forall \mathrm{v} \in \mathrm{V}, \quad (\mathsf{R}_{\mathcal{V}}(p))_{\mathrm{v}} := p(\mathrm{v}), \qquad \forall \mathrm{e} \in \mathrm{E}, \quad (\mathsf{R}_{\mathcal{E}}(\underline{u}))_{\mathrm{e}} := \int_{\mathrm{e}} \underline{u} \cdot \underline{\tau}_{\mathrm{e}}, \tag{3a}$$

$$\forall \mathrm{f} \in \mathrm{F}, \quad (\mathsf{R}_{\mathcal{F}}(\underline{\phi}))_{\mathrm{f}} := \int_{\mathrm{f}} \underline{\phi} \cdot \underline{\nu}_{\mathrm{f}}, \qquad \forall \mathrm{c} \in \mathrm{C}, \quad (\mathsf{R}_{\mathcal{C}}(s))_{\mathrm{c}} := \int_{\mathrm{c}} s, \tag{3b}$$

where $\underline{\tau}_{\mathrm{e}}$ is a unit tangent vector to edge e and $\underline{\nu}_{\mathrm{f}}$ is a unit normal vector to face f. The orientation of $\underline{\tau}_{\mathrm{e}}$ and that of $\underline{\nu}_{\mathrm{f}}$ is arbitrary, but fixed once and for all (more precisely, the orientation of f is fixed and determines the orientation of $\underline{\nu}_{\mathrm{f}}$). The definitions (3) are in agreement with the underlying physical nature of fields: a scalar potential field is discretized at vertices, a circulation at edges, a flux at faces, and a density at cells. The domain of the de Rham maps can be specified, e.g., using (broken) Sobolev spaces [see 34, 43].

In addition to the primal mesh, we introduce a dual mesh $\widetilde{\mathrm{M}} := \{\widetilde{\mathrm{V}}, \widetilde{\mathrm{E}}, \widetilde{\mathrm{F}}, \widetilde{\mathrm{C}}\}$, where $\widetilde{\mathrm{V}}$ collects dual vertices generically denoted $\tilde{\mathrm{v}}$, $\widetilde{\mathrm{E}}$ dual edges $\tilde{\mathrm{e}}$, $\widetilde{\mathrm{F}}$ dual faces $\tilde{\mathrm{f}}$, and $\widetilde{\mathrm{C}}$ dual cells $\tilde{\mathrm{c}}$. Contrary to the primal mesh, the dual mesh is not a cell complex because some part of the boundary of a k-cell, $1 \le k \le 3$, in $\widetilde{\mathrm{M}}$ is not in $\widetilde{\mathrm{M}}$ if this cell touches the boundary $\partial\Omega$. There are several ways to build a dual mesh, for instance using Voronoï diagrams or a barycentric subdivision [see 9]. The precise way $\widetilde{\mathrm{M}}$ is built is not needed at this stage. We only require that there is a one-to-one correspondence between primal vertices and dual cells, primal edges and dual faces, primal faces and dual edges, and primal cells and dual vertices. As a result, $\#\widetilde{\mathrm{V}} = \#\mathrm{C}$, $\#\widetilde{\mathrm{E}} = \#\mathrm{F}$, $\#\widetilde{\mathrm{F}} = \#\mathrm{E}$ and $\#\widetilde{\mathrm{C}} = \#\mathrm{V}$, where $\#\mathrm{X}$ denotes the cardinality of the set X. To stress this one-to-one pairing, we denote $\tilde{\mathrm{v}}(\mathrm{c}) \in \widetilde{\mathrm{V}}$ the dual vertex related to the primal cell $\mathrm{c} \in \mathrm{C}$, $\tilde{\mathrm{e}}(\mathrm{f}) \in \widetilde{\mathrm{E}}$ the dual edge related to the primal face $\mathrm{f} \in \mathrm{F}$, $\tilde{\mathrm{f}}(\mathrm{e}) \in \widetilde{\mathrm{F}}$ the dual face related to the primal edge $\mathrm{e} \in \mathrm{E}$, and $\tilde{\mathrm{c}}(\mathrm{v}) \in \widetilde{\mathrm{C}}$ the dual cell related to the primal vertex $\mathrm{v} \in \mathrm{V}$. The de Rham maps on the dual mesh act similarly to (3), with codomains denoted $\widetilde{\mathcal{V}}, \widetilde{\mathcal{E}}, \widetilde{\mathcal{F}}, \widetilde{\mathcal{C}}$. The orientation of the unit vector $\underline{\tau}_{\tilde{\mathrm{e}}(\mathrm{f})}$ is determined by $\underline{\nu}_{\mathrm{f}}$ for all $\mathrm{f} \in \mathrm{F}$ and that of $\underline{\nu}_{\tilde{\mathrm{f}}(\mathrm{e})}$ by $\underline{\tau}_{\mathrm{e}}$ for all $\mathrm{e} \in \mathrm{E}$. This means that we operate a transfer of orientation from the primal mesh to the dual mesh. Figure 1 illustrates primal and dual mesh entities.

The analysis of CDO schemes requires some regularity assumptions on the underlying meshes. A rather general way to assert the regularity of polyhedral meshes is the following assumption, which we denote ($\mathbf{H}_{\mathrm{M}}$) in what follows: There exists a matching simplicial submesh that is shape-regular in the usual sense and that is a common refinement of both primal and dual meshes with each primal and dual cell containing a uniformly bounded number of subsimplices. Moreover, we assume for simplicity that primal faces are planar.

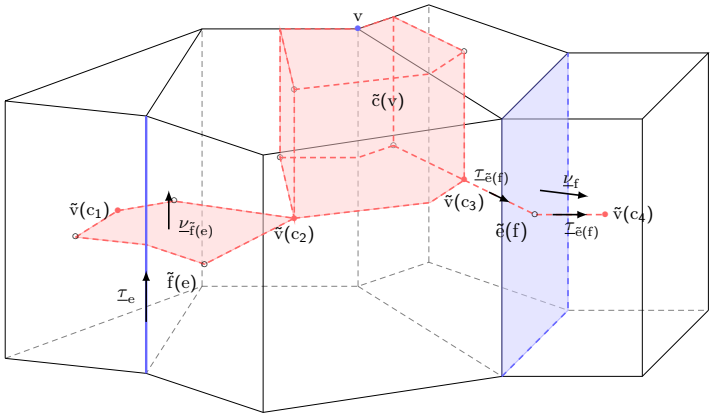

Figure 1: Examples of primal and dual mesh entities.

2.2 Discrete differential operators

The discrete differential operators on the primal mesh

$$\mathsf{GRAD} : \mathcal{V} \to \mathcal{E}, \qquad \mathsf{CURL} : \mathcal{E} \to \mathcal{F}, \qquad \mathsf{DIV} : \mathcal{F} \to \mathcal{C}, \tag{4a}$$

act such that, for all $\mathbf{p} \in \mathcal{V}$, $\mathbf{u} \in \mathcal{E}$ and $\boldsymbol{\phi} \in \mathcal{F}$,

$$\mathsf{GRAD}(\mathbf{p})|_e := \sum_{v \in V_e} \iota_{v,e} \mathbf{p}_v, \qquad \mathsf{CURL}(\mathbf{u})|_f := \sum_{e \in E_f} \iota_{e,f} \mathbf{u}_e, \qquad \mathsf{DIV}(\boldsymbol{\phi})|_c := \sum_{f \in F_c} \iota_{f,c} \boldsymbol{\phi}_f, \tag{4b}$$

where $V_e := \{v \in V \,|\, v \subset \partial e\}$ with $\iota_{v,e} = 1$ if $\underline{\tau}_e$ points towards v, $\iota_{v,e} = -1$ otherwise; $E_f := \{e \in E \,|\, e \subset \partial f\}$ with $\iota_{e,f} = 1$ if $\underline{\tau}_e$ shares the same orientation as that induced by $\underline{\nu}_f$, $\iota_{e,f} = -1$ otherwise; and $F_c := \{f \in F \,|\, f \subset \partial c\}$ with $\iota_{f,c} = 1$ if $\underline{\nu}_f$ points outward c, $\iota_{f,c} = -1$ otherwise. Algebraically, the discrete differential operators are represented by an incidence matrix (with entries in $\{0, \pm 1\}$). This reflects the topological or metric-free nature of these operators, which is a feature shared by many mimetic schemes; see e.g. [10, 16, 42, 8, 20, 28, 38]. The discrete differential operators commute with the de Rham maps,

$$\mathsf{R}_{\mathcal{E}}(\underline{\mathrm{grad}}) = \mathsf{GRAD}(\mathsf{R}_{\mathcal{V}}), \quad \mathsf{R}_{\mathcal{F}}(\underline{\mathrm{curl}}) = \mathsf{CURL}(\mathsf{R}_{\mathcal{E}}), \quad \mathsf{R}_{\mathcal{C}}(\mathrm{div}) = \mathsf{DIV}(\mathsf{R}_{\mathcal{F}}), \tag{5}$$

they produce a cochain complex,

$$\mathsf{CURL}(\mathsf{GRAD}) = 0_{\mathcal{F}}, \quad \mathsf{DIV}(\mathsf{CURL}) = 0_{\mathcal{C}}, \tag{6}$$

and, under assumption ($\mathbf{H}_{\boldsymbol{\Omega}}$), they generate an exact sequence,

$$\operatorname{Im} \mathsf{GRAD} = \operatorname{Ker} \mathsf{CURL}, \quad \operatorname{Im} \mathsf{CURL} = \operatorname{Ker} \mathsf{DIV}, \tag{7}$$

where Im is the range of an operator and Ker the kernel.

The discrete differential operators on the dual mesh

$$\widetilde{\mathsf{GRAD}} : \widetilde{\mathcal{V}} \to \widetilde{\mathcal{E}}, \qquad \widetilde{\mathsf{CURL}} : \widetilde{\mathcal{E}} \to \widetilde{\mathcal{F}}, \qquad \widetilde{\mathsf{DIV}} : \widetilde{\mathcal{F}} \to \widetilde{\mathcal{C}}, \tag{8}$$

are defined similarly to (4b). The discrete differential operators on the dual mesh commute with the de Rham maps on all interior dual mesh entities,

$$\mathsf{R}_{\widetilde{\mathcal{E}}}(\underline{\mathrm{grad}})|_{\tilde{e}} = \widetilde{\mathsf{GRAD}}(\mathsf{R}_{\widetilde{\mathcal{V}}})|_{\tilde{e}}, \quad \mathsf{R}_{\widetilde{\mathcal{F}}}(\underline{\mathrm{curl}})|_{\tilde{f}} = \widetilde{\mathsf{CURL}}(\mathsf{R}_{\widetilde{\mathcal{E}}})|_{\tilde{f}}, \quad \mathsf{R}_{\widetilde{\mathcal{C}}}(\mathrm{div})|_{\tilde{c}} = \widetilde{\mathsf{DIV}}(\mathsf{R}_{\widetilde{\mathcal{F}}})|_{\tilde{c}}, \tag{9}$$

for all $\tilde{\mathrm{e}}$, $\tilde{\mathrm{f}}$, and $\tilde{\mathrm{c}}$ which do not intersect the boundary $\partial\Omega$. Moreover, these operators produce a cochain complex,

$$\widetilde{\mathsf{CURL}}(\widetilde{\mathsf{GRAD}}) = 0_{\widetilde{\mathcal{F}}}, \quad \widetilde{\mathsf{DIV}}(\widetilde{\mathsf{CURL}}) = 0_{\widetilde{\mathcal{C}}}. \tag{10}$$

and, under assumption ($\mathbf{H_\Omega}$), they generate an exact sequence,

$$\operatorname{Im}\widetilde{\mathsf{GRAD}} = \operatorname{Ker}\widetilde{\mathsf{CURL}}, \quad \operatorname{Im}\widetilde{\mathsf{CURL}} = \operatorname{Ker}\widetilde{\mathsf{DIV}}. \tag{11}$$

The last important property is an adjunction between discrete differential operators on the primal and dual meshes. We define global duality products as follows:

$$\big[\!\big[\mathbf{p},\mathbf{s}\big]\!\big]_{\mathcal{V}\tilde{\mathcal{C}}} := \sum_{\mathrm{v}\in\mathrm{V}} \mathbf{p}_{\mathrm{v}}\mathbf{s}_{\tilde{\mathrm{c}}(\mathrm{v})}, \qquad \big[\!\big[\mathbf{u},\boldsymbol{\phi}\big]\!\big]_{\mathcal{E}\tilde{\mathcal{F}}} := \sum_{\mathrm{e}\in\mathrm{E}} \mathbf{u}_{\mathrm{e}}\boldsymbol{\phi}_{\tilde{\mathrm{f}}(\mathrm{e})}, \tag{12a}$$

$$\big[\!\big[\mathbf{s},\mathbf{p}\big]\!\big]_{\mathcal{C}\tilde{\mathcal{V}}} := \sum_{\mathrm{c}\in\mathrm{C}} \mathbf{s}_{\mathrm{c}}\mathbf{p}_{\tilde{\mathrm{v}}(\mathrm{c})}, \qquad \big[\!\big[\boldsymbol{\phi},\mathbf{u}\big]\!\big]_{\mathcal{F}\tilde{\mathcal{E}}} := \sum_{\mathrm{f}\in\mathrm{F}} \boldsymbol{\phi}_{\mathrm{f}}\mathbf{u}_{\tilde{\mathrm{e}}(\mathrm{f})}, \tag{12b}$$

for all $(\mathbf{p},\mathbf{s}) \in \mathcal{V}\times\widetilde{\mathcal{C}}$ and $(\mathbf{u},\boldsymbol{\phi}) \in \mathcal{E}\times\widetilde{\mathcal{F}}$ in (12a) and for all $(\mathbf{s},\mathbf{p}) \in \mathcal{C}\times\widetilde{\mathcal{V}}$ and $(\boldsymbol{\phi},\mathbf{u}) \in \mathcal{F}\times\widetilde{\mathcal{E}}$ in (12b). Then, the following identities hold:

$$\forall(\mathbf{p},\boldsymbol{\phi}) \in \mathcal{V}\times\widetilde{\mathcal{F}}, \qquad \big[\!\big[\mathsf{GRAD}(\mathbf{p}),\boldsymbol{\phi}\big]\!\big]_{\mathcal{E}\tilde{\mathcal{F}}} = -\big[\!\big[\mathbf{p},\widetilde{\mathsf{DIV}}(\boldsymbol{\phi})\big]\!\big]_{\mathcal{V}\tilde{\mathcal{C}}}, \tag{13a}$$

$$\forall(\mathbf{u},\boldsymbol{\omega}) \in \mathcal{E}\times\widetilde{\mathcal{E}}, \qquad \big[\!\big[\mathsf{CURL}(\mathbf{u}),\mathbf{v}\big]\!\big]_{\mathcal{F}\tilde{\mathcal{E}}} = \big[\!\big[\mathbf{u},\widetilde{\mathsf{CURL}}(\mathbf{v})\big]\!\big]_{\mathcal{E}\tilde{\mathcal{F}}}, \tag{13b}$$

$$\forall(\boldsymbol{\phi},\mathbf{p}) \in \mathcal{F}\times\widetilde{\mathcal{V}}, \qquad \big[\!\big[\mathsf{DIV}(\boldsymbol{\phi}),\mathbf{p}\big]\!\big]_{\mathcal{C}\tilde{\mathcal{V}}} = -\big[\!\big[\boldsymbol{\phi},\widetilde{\mathsf{GRAD}}(\mathbf{p})\big]\!\big]_{\mathcal{F}\tilde{\mathcal{E}}}. \tag{13c}$$

Algebraically, the matrix representing a discrete differential operator on the dual mesh is the transpose of that of the corresponding operator on the primal mesh.

2.3 Discrete Hodge operators

In the CDO framework, the crucial point is the design of the discrete Hodge operator. This operator is related to the discretization of a constitutive relation, and in contrast to discrete differential operators, its design is not uniquely defined. The discrete Hodge operator maps DoFs attached to primal mesh entities to DoFs attached to the corresponding dual mesh entities in one-to-one pairing, and is algebraically represented by a (square) symmetric positive definite (SPD) matrix. A generic discrete Hodge operator is denoted $\mathsf{H}_\alpha^{\chi\tilde{\mathcal{Y}}}$ with ${}_{\chi}\tilde{\mathcal{Y}} \in \{{}_{\mathcal{V}}\tilde{\mathcal{C}}, {}_{\mathcal{E}}\tilde{\mathcal{F}}, {}_{\mathcal{F}}\tilde{\mathcal{E}}, {}_{\mathcal{C}}\tilde{\mathcal{V}}\}$ and where α refers to the material property involved in the constitutive relation. The set of primal (resp., dual) mesh entities associated with $\mathcal{X}$ (resp., $\widetilde{\mathcal{Y}}$) is denoted X (resp., $\widetilde{\mathrm{Y}}$).

In the context of the Stokes equations, the two most salient discrete Hodge operators are $\mathsf{H}_\alpha^{\mathcal{E}\tilde{\mathcal{F}}}$ and $\mathsf{H}_\alpha^{\mathcal{F}\tilde{\mathcal{E}}}$, so that we focus on the case where ${}_{\chi}\tilde{\mathcal{Y}} \in \{{}_{\mathcal{E}}\tilde{\mathcal{F}}, {}_{\mathcal{F}}\tilde{\mathcal{E}}\}$. These operators are assembled from local discrete Hodge operators attached to primal cells. Let $\mathrm{c} \in \mathrm{C}$. We introduce the local subsets

$$\mathrm{X}_\mathrm{c} := \{\mathrm{x}\in\mathrm{X} \,|\, \mathrm{x}\subseteq\partial\mathrm{c}\}, \qquad \widetilde{\mathrm{Y}}_\mathrm{c} := \{\tilde{\mathrm{y}}_\mathrm{c}(\mathrm{x}) := \tilde{\mathrm{y}}(\mathrm{x})\cap\mathrm{c},\ \mathrm{x}\in\mathrm{X}_\mathrm{c}\}. \tag{14}$$

In particular, we need the local subsets $\mathrm{E}_\mathrm{c} := \{\mathrm{e}\in\mathrm{E} \,|\, \mathrm{e}\subset\partial\mathrm{c}\}$ and $\widetilde{\mathrm{F}}_\mathrm{c} := \{\tilde{\mathrm{f}}_\mathrm{c}(\mathrm{e}) := \tilde{\mathrm{f}}(\mathrm{e})\cap\mathrm{c} \,|\, \mathrm{e}\in\mathrm{E}_\mathrm{c}\}$, and $\mathrm{F}_\mathrm{c} := \{\mathrm{f}\in\mathrm{F} \,|\, \mathrm{f}\subset\partial\mathrm{c}\}$ and $\widetilde{\mathrm{E}}_\mathrm{c} := \{\tilde{\mathrm{e}}_\mathrm{c}(\mathrm{f}) := \tilde{\mathrm{e}}(\mathrm{f})\cap\mathrm{c} \,|\, \mathrm{f}\in\mathrm{F}_\mathrm{c}\}$. The local de Rham maps $\mathsf{R}_{\mathcal{X}_\mathrm{c}}$ mapping onto the space of local primal DoFs $\mathcal{X}_\mathrm{c}$ are defined as in (3), while the local de Rham maps $\mathsf{R}_{\widetilde{\mathcal{Y}}_\mathrm{c}}$ mapping onto the space of local dual DoFs $\widetilde{\mathcal{Y}}_\mathrm{c}$ are defined by restricting the domain of integration to c; for instance,

$$(\mathsf{R}_{\widetilde{\mathcal{E}}_\mathrm{c}}(\underline{u}))_{\tilde{\mathrm{e}}_\mathrm{c}(\mathrm{f})} := \int_{\tilde{\mathrm{e}}_\mathrm{c}(\mathrm{f})} \underline{u}\cdot\underline{\tau}_{\tilde{\mathrm{e}}_\mathrm{c}(\mathrm{f})}, \qquad (\mathsf{R}_{\widetilde{\mathcal{F}}_\mathrm{c}}(\underline{\phi}))_{\tilde{\mathrm{f}}_\mathrm{c}(\mathrm{e})} := \int_{\tilde{\mathrm{f}}_\mathrm{c}(\mathrm{e})} \underline{\phi}\cdot\underline{\nu}_{\tilde{\mathrm{f}}_\mathrm{c}(\mathrm{e})}, \tag{15}$$

where $\underline{\tau}_{\tilde{\mathrm{e}}_\mathrm{c}(\mathrm{f})}$ (resp., $\underline{\nu}_{\tilde{\mathrm{f}}_\mathrm{c}(\mathrm{e})}$) is consistently oriented by $\underline{\nu}_\mathrm{f}$ (resp., $\underline{\tau}_\mathrm{e}$). Then, the assembly of $\mathsf{H}_\alpha^{\chi\tilde{\mathcal{Y}}}$ can be written as

$$\mathsf{H}_\alpha^{\chi\tilde{\mathcal{Y}}} = \sum_{\mathrm{c}\in\mathrm{C}} \mathsf{P}_{\mathcal{X},\mathrm{c}}^* \cdot \mathsf{H}_\alpha^{\mathcal{X}_\mathrm{c}\tilde{\mathcal{Y}}_\mathrm{c}} \cdot \mathsf{P}_{\mathcal{X},\mathrm{c}}, \tag{16}$$

where $\mathsf{P}_{\mathcal{X},\mathrm{c}} : \mathcal{X} \to \mathcal{X}_\mathrm{c}$ is the (full-rank) map from global to local spaces of DoFs, $\mathsf{P}^*_{\mathcal{X},\mathrm{c}}$ the adjoint map, and $\mathsf{H}_\alpha^{\mathcal{X}_\mathrm{c}\widetilde{\mathcal{Y}}_\mathrm{c}} : \mathcal{X}_\mathrm{c} \to \widetilde{\mathcal{Y}}_\mathrm{c}$ the local discrete Hodge operator attached to the primal cell c. Observe that $\mathsf{H}_\alpha^{\mathcal{X}\widetilde{\mathcal{Y}}}$ is algebraically represented by a (large) sparse SPD matrix of order $\#\mathrm{X} = \#\widetilde{\mathrm{Y}}$, while $\mathsf{H}_\alpha^{\mathcal{X}_\mathrm{c}\widetilde{\mathcal{Y}}_\mathrm{c}}$ is algebraically represented by a (small) dense SPD matrix of order $\#\mathrm{X}_\mathrm{c} = \#\widetilde{\mathrm{Y}}_\mathrm{c}$.

The local discrete Hodge operators $\mathsf{H}_\alpha^{\mathcal{X}_\mathrm{c}\widetilde{\mathcal{Y}}_\mathrm{c}}$ must fulfill, for all $\mathrm{c} \in \mathrm{C}$, two key properties: stability and consistency; see [9]. To state these properties, we introduce some notation. Similarly to (12), we define local duality products as $[\![\mathbf{a}, \mathbf{b}]\!]_{\mathcal{X}_\mathrm{c}\widetilde{\mathcal{Y}}_\mathrm{c}} := \sum_{\mathrm{x}\in\mathrm{X}_\mathrm{c}} \mathbf{a}_\mathrm{x}\mathbf{b}_{\widetilde{\mathrm{y}}_\mathrm{c}(\mathrm{x})}$ for all $(\mathbf{a}, \mathbf{b}) \in \mathcal{X}_\mathrm{c}\times\widetilde{\mathcal{Y}}_\mathrm{c}$. We introduce the local mesh-dependent norm

$$\forall \mathbf{a} \in \mathcal{X}_\mathrm{c}, \qquad |\!|\!|\mathbf{a}|\!|\!|^2_{2,\mathcal{X}_\mathrm{c}} := \sum_{\mathrm{x}\in\mathrm{X}_\mathrm{c}} |\mathfrak{p}_{\mathrm{x},\mathrm{c}}| \left(\frac{\mathbf{a}_\mathrm{x}}{|\mathrm{x}|}\right)^2, \tag{17}$$

where $\mathfrak{p}_{\mathrm{x},\mathrm{c}}$ denotes a subvolume of c attached to the primal mesh entity x. There are several possible definitions for these subvolumes; an example is presented in Figure 2 for vertices, edges, and faces using a barycentric subdivision of an hexahedral cell. Observe that owing to mesh regularity, see ($\mathbf{H}_\mathrm{M}$), the

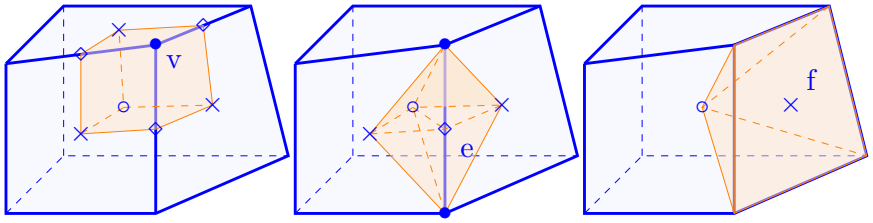

Figure 2: Hexahedral mesh cell c. Left: Example for $\mathfrak{p}_{\mathrm{v},\mathrm{c}}$; Middle: Example for $\mathfrak{p}_{\mathrm{e},\mathrm{c}}$; Right: Example for $\mathfrak{p}_{\mathrm{f},\mathrm{c}}$.

measure of $\mathfrak{p}_{\mathrm{x},\mathrm{c}}$ is uniformly equivalent to h_c^3, where h_c denotes the diameter of c. Then, the stability and consistency properties of the local discrete Hodge operators assert that, for all $\mathrm{c} \in \mathrm{C}$,

($\mathbf{A}1$) [Stability] There exists $\eta_\alpha > 0$ such that

$$\forall \mathbf{a} \in \mathcal{X}_\mathrm{c}, \quad \eta_\alpha |\!|\!|\mathbf{a}|\!|\!|^2_{2,\mathcal{X}_\mathrm{c}} \le [\![\mathbf{a}, \mathsf{H}_\alpha^{\mathcal{X}_\mathrm{c}\widetilde{\mathcal{Y}}_\mathrm{c}}(\mathbf{a})]\!]_{\mathcal{X}_\mathrm{c}\widetilde{\mathcal{Y}}_\mathrm{c}} \le \eta_\alpha^{-1} |\!|\!|\mathbf{a}|\!|\!|^2_{2,\mathcal{X}_\mathrm{c}}. \tag{18}$$

($\mathbf{A}2$) [$\mathbb{P}_0$-consistency] The local commuting operator $\lfloor\alpha, {}_{\mathcal{X}_\mathrm{c}}\widetilde{\mathcal{Y}}_\mathrm{c}\rceil(\bullet) := \mathsf{H}_\alpha^{\mathcal{X}_\mathrm{c}\widetilde{\mathcal{Y}}_\mathrm{c}} \cdot \mathsf{R}_{\mathcal{X}_\mathrm{c}}(\bullet) - \mathsf{R}_{\widetilde{\mathcal{Y}}_\mathrm{c}}(\alpha\bullet)$ satisfies $\lfloor\alpha, {}_{\mathcal{X}_\mathrm{c}}\widetilde{\mathcal{Y}}_\mathrm{c}\rceil(\underline{C}) = 0$ for all $\underline{C}$ constant in c.

These two properties share the same spirit as those introduced for MFD schemes by [12, 14]. One way to design local discrete Hodge operators matching these two properties is to define them as local mass matrices built from reconstruction functions satisfying suitable properties inspired from the Discrete Geometric Approach (DGA) approach of [17]; see [9].

2.4 Discrete functional analysis

We introduce global mesh-dependent norms by summing cellwise the local mesh-dependent norms defined by (17), i.e., $|\!|\!|\mathbf{a}|\!|\!|^2_{2,\mathcal{X}} := \sum_{\mathrm{c}\in\mathrm{C}} |\!|\!|\mathsf{P}_{\mathcal{X}_\mathrm{c}}(\mathbf{a})|\!|\!|^2_{2,\mathcal{X}_\mathrm{c}}$. Summing cellwise ($\mathbf{A}1$) and using (16), we infer that

$$\forall \mathbf{a} \in \mathcal{X}, \qquad \eta_\alpha |\!|\!|\mathbf{a}|\!|\!|^2_{2,\mathcal{X}} \le |\!|\!|\mathbf{a}|\!|\!|^2_\alpha := [\![\mathbf{a}, \mathsf{H}_\alpha^{\mathcal{X}\widetilde{\mathcal{Y}}}(\mathbf{a})]\!]_{\mathcal{X}\widetilde{\mathcal{Y}}} \le \eta_\alpha^{-1} |\!|\!|\mathbf{a}|\!|\!|^2_{2,\mathcal{X}}. \tag{19}$$

The following two discrete Poincaré inequalities are important tools for the analysis of CDO schemes applied to the Stokes equations. We postpone their proof to Appendix A. The discrete Hodge operator $\mathsf{H}_1^{\mathcal{V}^c}$ in Lemma 2.1 is diagonal with entries equal to $|\tilde{\mathrm{c}}(\mathrm{v})|$, while the discrete Hodge operator $\mathsf{H}_\alpha^{\mathcal{E}\widetilde{\mathcal{F}}}$ in Lemma 2.2 only needs to satisfy the stability property ($\mathbf{A}1$). Similar Poincaré inequalities are derived in [4] for conforming discrete functions in the corresponding functional spaces. The difference is that

the present inequalities hold on the spaces of DoFs and that the orthogonality is stated using a discrete Hodge operator; even if this operator is devised from local reconstruction functions, the latter need not be conforming.

Lemma 2.1 (Discrete Poincaré–Wirtinger inequality). *Assume ($\mathbf{H}_{\mathrm{M}}$). Then, there exists $C_{\mathrm{P}}^{(0)}$ (independent of the mesh size, but dependent on mesh regularity) such that, for all $\mathbf{p} \in \mathcal{V}$ verifying $\left[\!\left[\mathbf{p}, \mathsf{H}_1^{\mathcal{V}\tilde{\mathcal{C}}}(\mathbf{1})\right]\!\right]_{\mathcal{V}\tilde{\mathcal{C}}} = 0$, the following inequality holds:*

$$\|\mathbf{p}\|_{2,\mathcal{V}} \le C_{\mathrm{P}}^{(0)} \|\mathsf{GRAD}(\mathbf{p})\|_{2,\mathcal{E}}. \tag{20}$$

Lemma 2.2 (Discrete Poincaré inequality for the curl). *Assume ($\mathbf{H}_{\mathrm{M}}$) and ($\mathbf{H}_{\mathbf{\Omega}}$). Let $\mathsf{H}_\alpha^{\mathcal{E}\tilde{\mathcal{F}}}$ satisfy ($\mathbf{A}1$). Then, there exists $C_{\mathrm{P}}^{(1)}$ (independent of the mesh size, but dependent on mesh regularity and the stability constant η_α) such that, for all $\mathbf{u} \in \mathcal{E}$ such that $\left[\!\left[\mathbf{u}, \mathsf{H}_\alpha^{\mathcal{E}\tilde{\mathcal{F}}}(\mathbf{v})\right]\!\right]_{\mathcal{E}\tilde{\mathcal{F}}} = 0$ for all $\mathbf{v} \in \operatorname{Ker}\mathsf{CURL}$, the following inequality holds:*

$$\|\mathbf{u}\|_{2,\mathcal{E}} \le C_{\mathrm{P}}^{(1)} \|\mathsf{CURL}(\mathbf{u})\|_{2,\mathcal{F}}. \tag{21}$$

2.5 Bound on consistency error

In CDO schemes, the discrete errors are bounded only by the consistency error introduced by the lack of commuting property of the discrete Hodge operators with the de Rahm maps; see [10], [29], [18], and [9]. Recalling ($\mathbf{A}2$), the global commuting operators are defined as follows:

$$\lfloor \alpha,\, {}_{\mathcal{X}}\tilde{\mathcal{Y}} \rceil(\bullet) := \mathsf{H}_\alpha^{\mathcal{X}\tilde{\mathcal{Y}}} \cdot \mathsf{R}_{\mathcal{X}}(\bullet) - \mathsf{R}_{\tilde{\mathcal{Y}}}(\alpha\bullet). \tag{22}$$

We define the discrete norm such that $\|\mathbf{b}\|_{(\alpha)^{-1}}^2 := \left[\!\left[(\mathsf{H}_\alpha^{\mathcal{X}\tilde{\mathcal{Y}}})^{-1}(\mathbf{b}), \mathbf{b}\right]\!\right]_{\mathcal{X}\tilde{\mathcal{Y}}}$ for all $\mathbf{b} \in \widetilde{\mathcal{Y}}$.

In what follows, we abbreviate $A \lesssim B$ the inequality $A \le cB$ with positive constant c whose value can change at each occurrence and is independent of any mesh size (but can depend on the mesh regularity and the stability constants of the discrete Hodge operators). Let $H^1(\mathrm{C})$ denote the broken Sobolev space H^1 on the primal mesh. Let $h_{\mathrm{M}} := \max_{\mathrm{c}\in\mathrm{C}} h_c$ denote the maximal mesh size. We now derive a first-order estimate on the consistency error for smooth enough vector fields.

Lemma 2.3 (Error bound for smooth fields). *Assume ($\mathbf{H}_{\mathrm{M}}$). Let $\underline{b} \in H^1(\mathrm{C})^3$ be such that $\underline{\mathrm{curl}}(\underline{b}) \in L^4(\Omega)^3$. Let $\mathsf{H}_\alpha^{\mathcal{X}\tilde{\mathcal{Y}}}$ satisfy ($\mathbf{A}1$) and ($\mathbf{A}2$) with ${}_{\mathcal{X}}\tilde{\mathcal{Y}} = \mathcal{E}\tilde{\mathcal{F}}$ or ${}_{\mathcal{F}}\tilde{\mathcal{E}}$. Then, the following inequality holds:*

$$\|\lfloor \alpha,\, {}_{\mathcal{X}}\tilde{\mathcal{Y}} \rceil(\underline{b})\|_{(\alpha)^{-1}}^2 \lesssim h_{\mathrm{M}}^2 \left(\|\underline{b}\|_{H^1(\mathrm{C})^3}^2 + \|\underline{\mathrm{curl}}\,\underline{b}\|_{L^4(\Omega)^3}^2 \right). \tag{23}$$

Proof. We preliminarily observe that the smoothness assumption on $\underline{b}$ entails that this vector field is in the domain of the de Rahm maps $\mathsf{R}_{\mathcal{E}}$, $\mathsf{R}_{\mathcal{F}}$, $\mathsf{R}_{\tilde{\mathcal{E}}}$ and $\mathsf{R}_{\tilde{\mathcal{F}}}$; see in particular [34]. We only prove (23) for ${}_{\mathcal{X}}\tilde{\mathcal{Y}} = \mathcal{E}\tilde{\mathcal{F}}$, the proof for ${}_{\mathcal{X}}\tilde{\mathcal{Y}} = \mathcal{F}\tilde{\mathcal{E}}$ being similar. The proof follows the same lines as [9, Theorem 3.3]. Using the algebraic result of [18, Theorem 9] yields $\|\lfloor \alpha,\, \mathcal{E}\tilde{\mathcal{F}} \rceil(\underline{b})\|_{(\alpha)^{-1}}^2 \le \sum_{\mathrm{c}\in\mathrm{C}} (T_{\mathrm{c}})^2$ where $(T_{\mathrm{c}})^2 := \|\lfloor \alpha,\, \mathcal{E}_{\mathrm{c}}\tilde{\mathcal{F}}_{\mathrm{c}} \rceil(\underline{b})\|_{(\alpha)^{-1},\mathrm{c}}^2$ with $\|\mathbf{b}\|_{(\alpha)^{-1},\mathrm{c}}^2 := \left[\!\left[(\mathsf{H}_\alpha^{\mathcal{E}_{\mathrm{c}}\tilde{\mathcal{F}}_{\mathrm{c}}})^{-1}(\mathbf{b}), \mathbf{b}\right]\!\right]_{\mathcal{E}_{\mathrm{c}}\tilde{\mathcal{F}}_{\mathrm{c}}}$ for all $\mathbf{b} \in \widetilde{\mathcal{F}}_{\mathrm{c}}$. Then, owing to ($\mathbf{A}1$), ($\mathbf{A}2$), the triangle inequality, and ($\mathbf{H}_{\mathrm{M}}$), we infer that

$$(T_{\mathrm{c}})^2 = \|\lfloor \alpha,\, \mathcal{E}_{\mathrm{c}}\tilde{\mathcal{F}}_{\mathrm{c}} \rceil((\underline{b} - \underline{B})|_{\mathrm{c}})\|_{(\alpha)^{-1},\mathrm{c}}^2 \lesssim h_{\mathrm{c}} \sum_{\mathrm{e}\in\mathrm{E}_{\mathrm{c}}} |T_{\mathrm{e}}|^2 + h_{\mathrm{c}}^{-1} \sum_{\mathrm{e}\in\mathrm{E}} |T_{\tilde{\mathrm{f}}_{\mathrm{c}}(\mathrm{e})}|^2,$$

where $T_{\tilde{\mathrm{f}}_{\mathrm{c}}(\mathrm{e})} := \int_{\tilde{\mathrm{f}}_{\mathrm{c}}(\mathrm{e})} (\underline{b} - \underline{B}) \cdot \underline{\nu}_{\tilde{\mathrm{f}}_{\mathrm{c}}(\mathrm{e})}$, $T_{\mathrm{e}} := \int_{\mathrm{e}} (\underline{b} - \underline{B}) \cdot \underline{\tau}_{\mathrm{e}}$, and $\underline{B}$ is the piecewise constant approximation of $\underline{b}$ on the primal mesh. Using mesh regularity and approximation results, we finally obtain that $|T_{\tilde{\mathrm{f}}_{\mathrm{c}}(\mathrm{e})}|^2 \lesssim h_{\mathrm{c}}^3 \|\underline{b}\|_{H^1(\mathrm{c})^3}^2$ and $|T_{\mathrm{e}}|^2 \lesssim h_{\mathrm{c}} \left(\|\underline{b}\|_{H^1(\mathrm{c})^3}^2 + \|\underline{\mathrm{curl}}\,\underline{b}\|_{L^4(\mathrm{c})}^2 \right)$; see [2, Lemma 4.7] applied with $p = 4$. □

3 Vertex-Based Pressure Schemes

3.1 Discrete systems

In vertex-based pressure schemes, the starting formulation is the 2-field curl formulation (1). Although the mass density ρ and the viscosity μ are constant, we rewrite (1) using these material properties so as to identify where a discrete Hodge operator should be used. We obtain

$$\begin{cases} \underline{\mathrm{curl}}(\mu\,\underline{\mathrm{curl}}(\underline{u})) + \rho\,\underline{\mathrm{grad}}(p^*) = \rho\underline{f}, & \text{in } \Omega, \\ \mathrm{div}(\rho\underline{u}) = 0, & \text{in } \Omega, \end{cases} \tag{24}$$

where we have introduced the pressure potential $p^* := \frac{p}{\rho}$. We focus on natural BCs for (24), which are given by

$$\rho\underline{u}\cdot\underline{\nu}_{\partial\Omega} = u_\nu^{\mathrm{bc}}, \quad \mu\underline{\omega}\times\underline{\nu}_{\partial\Omega} = \underline{\omega}_\tau^{\mathrm{bc}}, \qquad \text{on } \partial\Omega, \tag{25}$$

with data u_ν^{bc} and $\underline{\omega}_\tau^{\mathrm{bc}}$; for essential BCs, see Remark 3.1. In what follows, we also consider the mass flux $\underline{\phi} := \rho\underline{u}$, the vorticity $\underline{\omega} = \underline{\mathrm{curl}}(\underline{u})$, and the auxiliary field $\underline{\omega}^* := \mu\underline{\omega}$ to which we loosely refer as viscous stress circulation. With these quantities, (24) can be rewritten as $\underline{\mathrm{curl}}(\underline{\omega}^*) + \rho\,\underline{\mathrm{grad}}(p^*) = \rho\underline{f}$ and $\mathrm{div}(\underline{\phi}) = 0$ in Ω.

In vertex-based pressure schemes, the two unknowns are the pressure potential p^* and the velocity $\underline{u}$. The DoFs of the pressure potential, denoted $\mathbf{p}^*$, are located at primal vertices. The DoFs of the velocity, denoted $\mathbf{u}$, are located at primal edges. The velocity field is therefore seen as a circulation. The vorticity DoFs, which are located at primal faces, are directly obtained from the velocity DoFs by setting $\boldsymbol{\omega} := \mathsf{CURL}(\mathbf{u})$. The translational invariance of the discrete pressure potential is fixed by the condition

$$\big[\!\big[\mathbf{p}^*, \mathsf{H}_1^{\mathcal{V}\widetilde{\mathcal{C}}}(\mathbf{1})\big]\!\big]_{\mathcal{V}\widetilde{\mathcal{C}}} = 0, \tag{26}$$

where $\mathsf{H}_1^{\mathcal{V}\widetilde{\mathcal{C}}}$ is defined before Lemma 2.1 and $\mathbf{1}\in\mathcal{V}$ has entries equal to 1, so that (26) can be rewritten as $\sum_{\mathrm{v}\in\mathrm{V}}|\tilde{\mathrm{c}}(\mathrm{v})|\mathbf{p}^*_{\mathrm{v}} = 0$, which is the discrete counterpart of the zero mean-value condition on the pressure.

There are two discrete Hodge operators, one related to the mass density ρ and the other to the viscosity μ. The discrete Hodge operator $\mathsf{H}_\rho^{\mathcal{E}\widetilde{\mathcal{F}}}$ allows us to define the discrete mass flux $\boldsymbol{\phi} := \mathsf{H}_\rho^{\mathcal{E}\widetilde{\mathcal{F}}}(\mathbf{u})$ located at dual faces (compare with $\underline{\phi} = \rho\underline{u}$), and the discrete Hodge operator $\mathsf{H}_\mu^{\mathcal{F}\widetilde{\mathcal{E}}}$ the discrete viscous stress circulation $\boldsymbol{\omega}^* := \mathsf{H}_\mu^{\mathcal{F}\widetilde{\mathcal{E}}}(\boldsymbol{\omega})$ located at dual edges (compare with $\underline{\omega}^* := \mu\underline{\omega}$). Both discrete Hodge operators are assumed to satisfy the stability and consistency properties (**A**1) and (**A**2). In what follows, we consider the following discrete norms:

$$\|\mathbf{u}\|_\rho^2 := \big[\!\big[\mathbf{u}, \mathsf{H}_\rho^{\mathcal{E}\widetilde{\mathcal{F}}}(\mathbf{u})\big]\!\big]_{\mathcal{E}\widetilde{\mathcal{F}}}, \qquad \|\boldsymbol{\phi}\|_{(\rho)^{-1}}^2 := \big[\!\big[(\mathsf{H}_\rho^{\mathcal{E}\widetilde{\mathcal{F}}})^{-1}(\boldsymbol{\phi}), \boldsymbol{\phi}\big]\!\big]_{\mathcal{E}\widetilde{\mathcal{F}}}, \tag{27a}$$

$$\|\boldsymbol{\omega}\|_\mu^2 := \big[\!\big[\boldsymbol{\omega}, \mathsf{H}_\mu^{\mathcal{F}\widetilde{\mathcal{E}}}(\boldsymbol{\omega})\big]\!\big]_{\mathcal{F}\widetilde{\mathcal{E}}}, \qquad \|\boldsymbol{\omega}^*\|_{(\mu)^{-1}}^2 := \big[\!\big[(\mathsf{H}_\mu^{\mathcal{F}\widetilde{\mathcal{E}}})^{-1}(\boldsymbol{\omega}^*), \boldsymbol{\omega}^*\big]\!\big]_{\mathcal{F}\widetilde{\mathcal{E}}}, \tag{27b}$$

for all $\mathbf{u}\in\mathcal{E}$, $\boldsymbol{\phi}\in\widetilde{\mathcal{F}}$, $\boldsymbol{\omega}\in\mathcal{F}$, and $\boldsymbol{\omega}^*\in\widetilde{\mathcal{E}}$. Owing to the Cauchy–Schwarz inequality, we infer that

$$\big[\!\big[\mathbf{u},\boldsymbol{\phi}\big]\!\big]_{\mathcal{E}\widetilde{\mathcal{F}}} \le \|\mathbf{u}\|_\rho\,\|\boldsymbol{\phi}\|_{(\rho)^{-1}}, \qquad \big[\!\big[\boldsymbol{\omega},\boldsymbol{\omega}^*\big]\!\big]_{\mathcal{F}\widetilde{\mathcal{E}}} \le \|\boldsymbol{\omega}\|_\mu\,\|\boldsymbol{\omega}^*\|_{(\mu)^{-1}}. \tag{28}$$

We introduce the following operators:

$$\begin{aligned} &\mathsf{A}^{\mathsf{vb}} : \mathcal{E}\to\widetilde{\mathcal{F}}, && \mathsf{B} : \mathcal{E}\to\widetilde{\mathcal{C}}, && \mathsf{B}^{\mathrm{T}} : \mathcal{V}\to\widetilde{\mathcal{F}}, \\ &\mathsf{A}^{\mathsf{vb}} := \widetilde{\mathsf{CURL}}\cdot\mathsf{H}_\mu^{\mathcal{F}\widetilde{\mathcal{E}}}\cdot\mathsf{CURL}, && \mathsf{B} := -\widetilde{\mathsf{DIV}}\cdot\mathsf{H}_\rho^{\mathcal{E}\widetilde{\mathcal{F}}}, && \mathsf{B}^{\mathrm{T}} := \mathsf{H}_\rho^{\mathcal{E}\widetilde{\mathcal{F}}}\cdot\mathsf{GRAD}. \end{aligned} \tag{29}$$

The operators B and B^{T} are indeed adjoint, and A^{vb} is selfadjoint owing to the selfadjointness of $\mathsf{H}_\rho^{\mathcal{E}\widetilde{\mathcal{F}}}$ and the discrete adjunction of GRAD and $\widetilde{\mathsf{DIV}}$ and that of CURL and $\widetilde{\mathsf{CURL}}$.

The vertex-based pressure scheme with homogeneous natural BCs is: Find $(\mathbf{p}^*,\mathbf{u})\in\mathcal{V}_{\perp\mathbf{1}}\times\mathcal{E}$, with $\mathcal{V}_{\perp\mathbf{1}} := \{\boldsymbol{\theta}\in\mathcal{V};\ \big[\!\big[\boldsymbol{\theta}, \mathsf{H}_1^{\mathcal{V}\widetilde{\mathcal{C}}}(\mathbf{1})\big]\!\big]_{\mathcal{V}\widetilde{\mathcal{C}}} = 0\}$, such that

$$\begin{pmatrix} \mathsf{A}^{\mathsf{vb}} & \mathsf{B}^{\mathrm{T}} \\ \mathsf{B} & 0 \end{pmatrix}\begin{pmatrix} \mathbf{u} \\ \mathbf{p}^* \end{pmatrix} = \begin{pmatrix} \mathsf{S}^{\mathsf{vb}}(\rho,\underline{f}) \\ 0_{\widetilde{\mathcal{C}}} \end{pmatrix}. \tag{30}$$

The right-hand side $\mathsf{S}^{\mathsf{vb}}(\rho,\underline{f}) \in \widetilde{\mathcal{F}}$ discretizes the external load $\rho\underline{f}$. Two expressions are considered in the analysis, respectively termed discrete primal and dual load and defined as follows:

$$\mathsf{S}_{\mathsf{p}}^{\mathsf{vb}}(\rho,\underline{f})|_{\tilde{\mathsf{f}}(\mathrm{e})} := (\mathsf{H}_{\rho}^{\mathcal{E}\tilde{\mathcal{F}}} \cdot \mathsf{R}_{\mathcal{E}}(\underline{f}))|_{\tilde{\mathsf{f}}(\mathrm{e})}, \qquad \mathsf{S}_{\mathsf{d}}^{\mathsf{vb}}(\rho,\underline{f})|_{\tilde{\mathsf{f}}(\mathrm{e})} := \mathsf{R}_{\widetilde{\mathcal{F}}}(\rho\underline{f})|_{\tilde{\mathsf{f}}(\mathrm{e})}, \qquad \forall \mathrm{e} \in \mathrm{E}. \tag{31}$$

Furthermore, non-homogeneous natural BCs can be easily incorporated by modifying the right-hand side of (30) accordingly. We observe that in (30), mass balance holds in each dual cell and momentum balance at each dual face. All the relations involved in (30) are summarized in Figure 3.

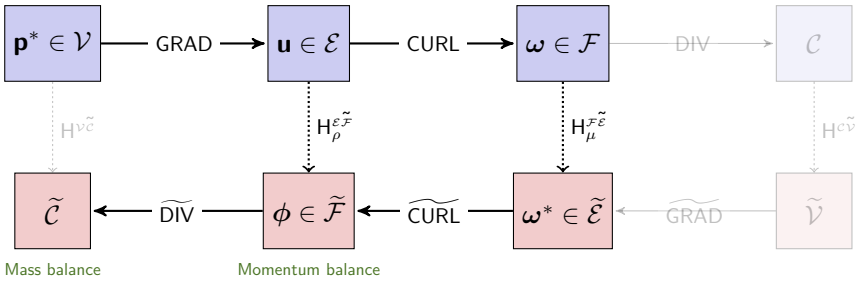

Figure 3: Tonti diagram of the vertex-based pressure scheme for the Stokes equations.

Remark 3.1 (Essentials BCs). Essential BCs for (24) are $\underline{u} \times \underline{\nu}_{\partial\Omega} = \underline{u}_{\tau}^{\mathrm{bc}}$ and $p^* = p^{\mathrm{bc}}$ on $\partial\Omega$. Such BCs can be enforced strongly by removing the corresponding DoFs from the discrete spaces or weakly by a (consistent) penalty method using the full spaces of DoFs. The analysis of vertex-based pressure schemes with essential BCs is left for future work; the main point consists of either deriving suitable discrete Poincaré inequalities on smaller spaces of DoFs if strong enforcement is considered or analyzing the consistency and penalty terms if weak enforcement is considered.

3.2 Stability and well-posedness

Owing to (**A**1) and recalling (19), the norms $\|\cdot\|_{2,\mathcal{E}}$ and $\|\cdot\|_{\rho}$ are uniformly equivalent on $\mathcal{E}$ (with respect to the mesh size); the same holds for the norms $\|\cdot\|_{2,\mathcal{F}}$ and $\|\cdot\|_{\mu}$ on $\mathcal{F}$. We equip the space $\mathcal{V}$ with the norm $\|\cdot\|_{2,\mathcal{V}}$ from Lemma 2.1 (obtained by summing cellwise the local norms (17) for vertices).

Lemma 3.1 (Coercivity). *Assume (*$\mathbf{H}_{\mathrm{M}}$*) and (*$\mathbf{H}_{\boldsymbol{\Omega}}$*). Then, there exists $\eta_{\mathsf{A}} > 0$ (independent of the mesh size) such that, for all $\mathbf{u} \in \operatorname{Ker}\mathsf{B}$, the following inequality holds:*

$$\left[\!\left[\mathbf{u}, \mathsf{A}^{\mathsf{vb}}(\mathbf{u})\right]\!\right]_{\mathcal{E}\tilde{\mathcal{F}}} \geq \eta_{\mathsf{A}} \|\mathbf{u}\|_{\rho}^2. \tag{32}$$

Proof. Let us verify that $\mathbf{u} \in \operatorname{Ker}\mathsf{B}$ implies that $\left[\!\left[\mathbf{u}, \mathsf{H}_{\rho}^{\mathcal{E}\tilde{\mathcal{F}}}(\mathbf{v})\right]\!\right]_{\mathcal{E}\tilde{\mathcal{F}}} = 0$ for all $\mathbf{v} \in \operatorname{Ker}\mathsf{CURL}$. Owing to ($\mathbf{H}_{\boldsymbol{\Omega}}$) and (7), there is $\boldsymbol{\theta} \in \mathcal{V}$ such that $\mathbf{v} = \mathsf{GRAD}(\boldsymbol{\theta})$. As a result,

$$\left[\!\left[\mathbf{u}, \mathsf{H}_{\rho}^{\mathcal{E}\tilde{\mathcal{F}}}(\mathbf{v})\right]\!\right]_{\mathcal{E}\tilde{\mathcal{F}}} = \left[\!\left[\mathbf{u}, \mathsf{B}^{\mathrm{T}}(\boldsymbol{\theta})\right]\!\right]_{\mathcal{E}\tilde{\mathcal{F}}} = \left[\!\left[\boldsymbol{\theta}, \mathsf{B}(\mathbf{u})\right]\!\right]_{\mathcal{V}\tilde{\mathcal{C}}} = 0.$$

Applying Lemma 2.2 and the stability property (19), we infer that

$$\eta_{\rho}^{-1}\|\mathbf{u}\|_{\rho}^2 \leq \|\mathbf{u}\|_{2,\mathcal{E}}^2 \leq (C_{\mathrm{P}}^{(1)})^2 \|\mathsf{CURL}(\mathbf{u})\|_{2,\mathcal{F}}^2 \leq (C_{\mathrm{P}}^{(1)})^2 \eta_{\mu}^{-1} \|\mathsf{CURL}(\mathbf{u})\|_{\mu}^2,$$

whence we infer (32) with $\eta_{\mathsf{A}} = \eta_{\rho}\eta_{\mu}(C_{\mathrm{P}}^{(1)})^{-2}$ since $\|\mathsf{CURL}(\mathbf{u})\|_{\mu}^2 = \left[\!\left[\mathbf{u}, \mathsf{A}^{\mathsf{vb}}(\mathbf{u})\right]\!\right]_{\mathcal{E}\tilde{\mathcal{F}}}$. □

Lemma 3.2 (Discrete inf-sup condition). *Assume (*$\mathbf{H}_{\mathrm{M}}$*). Then, there exists $\beta_{\mathsf{B}} > 0$ (independent of the mesh size) such that*

$$\inf_{\boldsymbol{\theta} \in \mathcal{V}_{\perp\mathbf{1}}} \sup_{\mathbf{u} \in \mathcal{E}} \frac{\left[\!\left[\boldsymbol{\theta}, \mathsf{B}(\mathbf{u})\right]\!\right]_{\mathcal{V}\tilde{\mathcal{C}}}}{\|\boldsymbol{\theta}\|_{2,\mathcal{V}} \|\mathbf{u}\|_{\rho}} \geq \beta_{\mathsf{B}}. \tag{33}$$

Proof. For all $\boldsymbol{\theta} \in \mathcal{V}_{\perp\mathbf{1}}$, set $\mathbf{u} := \mathsf{GRAD}(\boldsymbol{\theta})$. Then, $\big[\boldsymbol{\theta}, \mathsf{B}(\mathbf{u})\big]_{\mathcal{V}\widetilde{\mathcal{C}}} = \big[\mathbf{u}, \mathsf{B}^{\mathrm{T}}(\boldsymbol{\theta})\big]_{\mathcal{E}\widetilde{\mathcal{F}}} = \|\mathbf{u}\|_\rho^2$ and owing to Lemma 2.1 and (**A**1), we infer that $\|\boldsymbol{\theta}\|_{2,\mathcal{V}} \le C_{\mathrm{P}}^{(0)} \eta_\rho^{-1/2} \|\mathbf{u}\|_\rho$. This yields the inf-sup condition with $\beta_{\mathsf{B}} = \eta_\rho^{1/2} (C_{\mathrm{P}}^{(0)})^{-1}$. □

A classical consequence of Lemmata 3.1 and 3.2 is the following [13]:

Corollary 3.3 (Well-posedness)**.** *Assume (*$\mathbf{H}_{\mathrm{M}}$*) and (*$\mathbf{H}_{\boldsymbol{\Omega}}$*). Then, the discrete system* (30) *is well-posed.*

3.3 Error analysis for discrete dual load

Let $\underline{u}$, p^* solve the 2-field curl formulation (24) and recall that $\underline{\omega} = \underline{\mathrm{curl}}(\underline{u})$. Let $\mathbf{u}$, $\mathbf{p}^*$ solve the discrete system (30) and recall that $\boldsymbol{\omega} = \mathsf{CURL}(\mathbf{u})$. We define the following discrete errors:

$$\boldsymbol{\delta}\mathbf{p}^* := \mathsf{R}_{\mathcal{V}}(p^*) - \mathbf{p}^*, \quad \boldsymbol{\delta}\mathbf{u} := \mathsf{R}_{\mathcal{E}}(\underline{u}) - \mathbf{u}, \quad \boldsymbol{\delta}\boldsymbol{\omega} := \mathsf{R}_{\mathcal{F}}(\underline{\omega}) - \boldsymbol{\omega}. \tag{34}$$

Recall the global commuting operators $\lfloor \rho, {}_{\mathcal{E}}\widetilde{\mathcal{F}} \rceil(\bullet) := \mathsf{H}_\rho^{\mathcal{E}\widetilde{\mathcal{F}}} \cdot \mathsf{R}_{\mathcal{E}}(\bullet) - \mathsf{R}_{\widetilde{\mathcal{F}}}(\rho\bullet)$ and $\lfloor \mu, {}_{\mathcal{F}}\widetilde{\mathcal{E}} \rceil(\bullet) := \mathsf{H}_\mu^{\mathcal{F}\widetilde{\mathcal{E}}} \cdot \mathsf{R}_{\mathcal{F}}(\bullet) - \mathsf{R}_{\widetilde{\mathcal{E}}}(\mu\bullet)$. For simplicity, we assume that there are no quadrature errors when evaluating the external load.

Theorem 3.4 (Error bounds with discrete dual load)**.** *Let $\underline{u}$, p^* solve of the 2-field curl formulation* (24) *with homogeneous natural BCs. Let* $\mathbf{u}$, $\mathbf{p}^*$ *solve the discrete system* (30) *with the discrete dual load $\mathsf{S}_{\mathsf{d}}^{\mathsf{vb}}(\rho, \underline{f})$. Assume (*$\mathbf{H}_{\mathrm{M}}$*) and (*$\mathbf{H}_{\boldsymbol{\Omega}}$*). Then, the following error bounds hold:*

$$\|\mathsf{GRAD}(\boldsymbol{\delta}\mathbf{p}^*)\|_\rho \le \|\lfloor \rho, {}_{\mathcal{E}}\widetilde{\mathcal{F}} \rceil(\underline{\mathrm{grad}}(p^*))\|_{(\rho)^{-1}}, \tag{35a}$$

$$\|\boldsymbol{\delta}\boldsymbol{\omega}\|_\mu \lesssim \|\lfloor \rho, {}_{\mathcal{E}}\widetilde{\mathcal{F}} \rceil(\underline{\mathrm{grad}}(p^*))\|_{(\rho)^{-1}} + \|\lfloor \mu, {}_{\mathcal{F}}\widetilde{\mathcal{E}} \rceil(\underline{\omega})\|_{(\mu)^{-1}}, \tag{35b}$$

$$\|\boldsymbol{\delta}\mathbf{u}\|_\rho \lesssim \|\lfloor \rho, {}_{\mathcal{E}}\widetilde{\mathcal{F}} \rceil(\underline{\mathrm{grad}}(p^*))\|_{(\rho)^{-1}} + \|\lfloor \mu, {}_{\mathcal{F}}\widetilde{\mathcal{E}} \rceil(\underline{\omega})\|_{(\mu)^{-1}} + \|\lfloor \rho, {}_{\mathcal{E}}\widetilde{\mathcal{F}} \rceil(\underline{u})\|_{(\rho)^{-1}}. \tag{35c}$$

Moreover, if $\underline{u}, \underline{\omega}, \underline{\mathrm{grad}}(p^*) \in [H^1(\mathrm{C})]^3$ and $\underline{f} \in [L^4(\Omega)]^3$, the following error bounds hold:

$$\|\mathsf{GRAD}(\boldsymbol{\delta}\mathbf{p}^*)\|_\rho \lesssim h_{\mathrm{M}} \|\underline{\mathrm{grad}}(p^*)\|_{[H^1(\mathrm{C})]^3}, \tag{36a}$$

$$\|\boldsymbol{\delta}\boldsymbol{\omega}\|_\mu \lesssim h_{\mathrm{M}} \left(\|\underline{\mathrm{grad}}(p^*)\|_{[H^1(\mathrm{C})]^3} + \|\underline{\omega}\|_{[H^1(\mathrm{C})]^3} + \|\underline{f}\|_{[L^4(\Omega)]^3}\right), \tag{36b}$$

$$\|\boldsymbol{\delta}\mathbf{u}\|_\rho \lesssim h_{\mathrm{M}} \left(\|\underline{\mathrm{grad}}(p^*)\|_{[H^1(\mathrm{C})]^3} + \|\underline{\omega}\|_{[H^1(\mathrm{C})]^3} + \|\underline{f}\|_{[L^4(\Omega)]^3} + \|\underline{u}\|_{[H^1(\mathrm{C})]^3}\right). \tag{36c}$$

Proof. (1) We first derive the error equations. Applying $\mathsf{R}_{\widetilde{\mathcal{F}}}$ to the momentum and $\mathsf{R}_{\widetilde{\mathcal{C}}}$ to the mass balance equation in (24) yields

$$\begin{aligned} \widetilde{\mathsf{CURL}}(\mathsf{R}_{\widetilde{\mathcal{E}}}(\mu\underline{\omega})) + \mathsf{R}_{\widetilde{\mathcal{F}}}(\rho\,\underline{\mathrm{grad}}(p^*)) &= \mathsf{S}_{\mathsf{d}}^{\mathsf{vb}}(\rho, \underline{f}), \\ \widetilde{\mathsf{DIV}}(\mathsf{R}_{\widetilde{\mathcal{F}}}(\rho\underline{u})) &= 0_{\widetilde{\mathcal{C}}}, \end{aligned}$$

owing to the commuting property (9) on the interior dual mesh entities and the homogeneous BCs (25) on the dual mesh entities touching the boundary $\partial\Omega$. Subtracting from the corresponding equation in (30) and introducing the global commuting operators leads to

$$\widetilde{\mathsf{CURL}} \cdot \mathsf{H}_\mu^{\mathcal{F}\widetilde{\mathcal{E}}}(\boldsymbol{\delta}\boldsymbol{\omega}) + \mathsf{H}_\rho^{\mathcal{E}\widetilde{\mathcal{F}}} \cdot \mathsf{GRAD}(\boldsymbol{\delta}\mathbf{p}^*) = \widetilde{\mathsf{CURL}}(\lfloor \mu, {}_{\mathcal{F}}\widetilde{\mathcal{E}} \rceil(\underline{\omega})) + \lfloor \rho, {}_{\mathcal{E}}\widetilde{\mathcal{F}} \rceil(\underline{\mathrm{grad}}(p^*)), \tag{37a}$$

$$\widetilde{\mathsf{DIV}} \cdot \mathsf{H}_\rho^{\mathcal{E}\widetilde{\mathcal{F}}}(\boldsymbol{\delta}\mathbf{u}) = \widetilde{\mathsf{DIV}}(\lfloor \rho, {}_{\mathcal{E}}\widetilde{\mathcal{F}} \rceil(\underline{u})), \tag{37b}$$

since $\mathsf{R}_{\mathcal{F}}(\underline{\omega}) = \mathsf{R}_{\mathcal{F}}(\underline{\mathrm{curl}}(\underline{u})) = \mathsf{CURL}(\mathsf{R}_{\mathcal{E}}(\underline{u}))$ and $\mathsf{R}_{\mathcal{E}}(\underline{\mathrm{grad}}(p^*)) = \mathsf{GRAD}(\mathsf{R}_{\mathcal{V}}(p^*))$.
(2) Bound on the pressure gradient. We take the duality product of (37a) with $\mathsf{GRAD}(\boldsymbol{\delta}\mathbf{p}^*)$. Since $\big[\!\big[\mathsf{GRAD}(\boldsymbol{\delta}\mathbf{p}^*), \widetilde{\mathsf{CURL}}(\mathbf{x})\big]\!\big]_{\mathcal{E}\widetilde{\mathcal{F}}} = \big[\!\big[\mathsf{CURL}(\mathsf{GRAD}(\boldsymbol{\delta}\mathbf{p}^*)), \mathbf{x}\big]\!\big]_{\mathcal{F}\widetilde{\mathcal{E}}} = 0$ for all $\mathbf{x} \in \widetilde{\mathcal{E}}$, we infer that $\|\mathsf{GRAD}(\boldsymbol{\delta}\mathbf{p}^*)\|_\rho^2 =$

$\big[\!\big[\mathsf{GRAD}(\boldsymbol{\delta p}^*), \lfloor \rho,\, \varepsilon^{\widetilde{\mathcal{F}}} \rceil(\underline{\mathrm{grad}}(p^*))\big]\!\big]_{\mathcal{E}^{\widetilde{\mathcal{F}}}}$, whence (35a) follows from the Cauchy–Schwarz inequality (28).
(3) Bound on the vorticity. We use the discrete Hodge decomposition

$$\mathcal{E} = \operatorname{Im}\mathsf{GRAD} \overset{\perp\mathsf{H}}{\oplus} (\operatorname{Ker}\mathsf{CURL})^{\perp\mathsf{H}}, \tag{38}$$

where $(\operatorname{Ker}\mathsf{CURL})^{\perp\mathsf{H}} := \{\mathbf{u} \in \mathcal{E};\ \big[\!\big[\mathbf{u}, \mathsf{H}_\rho^{\mathcal{E}\widetilde{\mathcal{F}}}(\mathbf{v})\big]\!\big]_{\mathcal{E}^{\widetilde{\mathcal{F}}}} = 0, \forall \mathbf{v} \in \operatorname{Ker}\mathsf{CURL}\}$, which results from the decomposition $\mathcal{E} = \operatorname{Im}\mathsf{GRAD} \overset{\perp\mathsf{H}}{\oplus} (\operatorname{Im}\mathsf{GRAD})^{\perp\mathsf{H}}$ and $\operatorname{Im}\mathsf{GRAD} = \operatorname{Ker}\mathsf{CURL}$ owing to $(\mathbf{H_\Omega})$ and (7). Using (38), we set $\boldsymbol{\delta u} = \mathsf{GRAD}(\boldsymbol{\delta\theta}) + \boldsymbol{\delta u}_\perp$ with $\boldsymbol{\delta\theta} \in \mathcal{V}$ and $\boldsymbol{\delta u}_\perp \in (\operatorname{Ker}\mathsf{CURL})^{\perp\mathsf{H}}$. Observe that $\mathsf{CURL}(\boldsymbol{\delta u}_\perp) = \mathsf{CURL}(\boldsymbol{\delta u}) = \boldsymbol{\delta\omega}$ and that $\|\boldsymbol{\delta u}_\perp\|_\rho \lesssim \|\boldsymbol{\delta\omega}\|_\mu$ owing to Lemma 2.2 and the stability of $\mathsf{H}_\rho^{\varepsilon\widetilde{\mathcal{F}}}$ and $\mathsf{H}_\mu^{\mathcal{F}\widetilde{\mathcal{E}}}$. We take the duality product of (37a) with $\boldsymbol{\delta u}_\perp$. Since $\big[\!\big[\boldsymbol{\delta u}_\perp, \mathsf{H}_\rho^{\varepsilon\widetilde{\mathcal{F}}} \cdot \mathsf{GRAD}(\boldsymbol{\delta p}^*)\big]\!\big]_{\mathcal{E}^{\widetilde{\mathcal{F}}}} = 0$, we infer that

$$\|\boldsymbol{\delta\omega}\|_\mu^2 = \big[\!\big[\boldsymbol{\delta\omega}, \lfloor \mu,\, \mathcal{F}^{\widetilde{\mathcal{E}}} \rceil(\underline{\omega})\big]\!\big]_{\mathcal{F}^{\widetilde{\mathcal{E}}}} + \big[\!\big[\boldsymbol{\delta u}_\perp, \lfloor \rho,\, \varepsilon^{\widetilde{\mathcal{F}}} \rceil(\underline{\mathrm{grad}}(p^*))\big]\!\big]_{\mathcal{E}^{\widetilde{\mathcal{F}}}}. \tag{39}$$

The estimate (35b) results from Cauchy–Schwarz inequalities and $\|\boldsymbol{\delta u}_\perp\|_\rho \lesssim \|\boldsymbol{\delta\omega}\|_\mu$.
(4) Bound on the velocity. Since $\|\boldsymbol{\delta u}\|_\rho^2 = \|\boldsymbol{\delta u}_\perp\|_\rho^2 + \|\mathsf{GRAD}(\boldsymbol{\delta\theta})\|_\rho^2$ and $\|\boldsymbol{\delta u}_\perp\|_\rho \lesssim \|\boldsymbol{\delta\omega}\|_\mu$, it remains to estimate $\|\mathsf{GRAD}(\boldsymbol{\delta\theta})\|_\rho$. We take the duality product of (37b) with $\boldsymbol{\delta\theta}$. Since $\big[\boldsymbol{\delta u}_\perp, \mathsf{H}_\rho^{\varepsilon\widetilde{\mathcal{F}}} \cdot \mathsf{GRAD}(\boldsymbol{\delta\theta})\big]\!\big]_{\mathcal{E}^{\widetilde{\mathcal{F}}}} = 0$, we infer that

$$\|\mathsf{GRAD}(\boldsymbol{\delta\theta})\|_\rho^2 = \big[\!\big[\mathsf{GRAD}(\boldsymbol{\delta\theta}), \mathsf{H}_\rho^{\mathcal{E}\widetilde{\mathcal{F}}}(\boldsymbol{\delta u})\big]\!\big]_{\mathcal{E}^{\widetilde{\mathcal{F}}}} = \big[\!\big[\mathsf{GRAD}(\boldsymbol{\delta\theta}), \lfloor \rho,\, \varepsilon^{\widetilde{\mathcal{F}}} \rceil(\underline{u})\big]\!\big]_{\mathcal{E}^{\widetilde{\mathcal{F}}}},$$

and the Cauchy–Schwarz inequality (28) yields $\|\mathsf{GRAD}(\boldsymbol{\delta\theta})\|_\rho \le \|\lfloor \rho,\, \varepsilon^{\widetilde{\mathcal{F}}} \rceil(\underline{u})\|_{(\rho)^{-1}}$.
(5) Finally, the error bounds for smooth solutions result from Lemma 2.3, observing in particular that $\underline{\mathrm{curl}}(\underline{\omega}) \in [L^4(\Omega)]^3$ since $\underline{\mathrm{curl}}(\underline{\omega}) = \underline{f} - \underline{\mathrm{grad}}(p^*)$, $\underline{f} \in [L^4(\Omega)]^3$, and $\underline{\mathrm{grad}}(p^*) \in [H^1(\mathrm{C})]^3$, and that $\underline{\mathrm{curl}}(\underline{u}) \in [L^4(\Omega)]^3$ since $\underline{\omega} = \underline{\mathrm{curl}}(\underline{u}) \in [H^1(\mathrm{C})]^3$. □

3.4 Error analysis for discrete primal load

Theorem 3.5 (Error bounds with discrete primal load)**.** *Let $\underline{u}$, p^* solve of the 2-field curl formulation* (24) *with homogeneous natural BCs. Let* $\mathbf{u}$, $\mathbf{p}^*$ *solve the discrete system* (30) *with the discrete primal load $\mathsf{S}_\mathsf{p}^\mathsf{vb}(\rho, \underline{f})$. Assume* $(\mathbf{H}_\mathrm{M})$ *and* $(\mathbf{H_\Omega})$*. Then, the following error bounds hold:*

$$\|\mathsf{GRAD}(\boldsymbol{\delta p}^*)\|_\rho \le \|\lfloor \rho,\, \varepsilon^{\widetilde{\mathcal{F}}} \rceil(\underline{\mathrm{curl}}(\underline{\omega}^*))\|_{(\rho)^{-1}}, \tag{40a}$$

$$\|\boldsymbol{\delta\omega}\|_\mu \lesssim \|\lfloor \rho,\, \varepsilon^{\widetilde{\mathcal{F}}} \rceil(\underline{\mathrm{curl}}(\underline{\omega}^*))\|_{(\rho)^{-1}} + \|\lfloor \mu,\, \mathcal{F}^{\widetilde{\mathcal{E}}} \rceil(\underline{\omega})\|_{(\mu)^{-1}}, \tag{40b}$$

$$\|\boldsymbol{\delta u}\|_\rho \lesssim \|\lfloor \rho,\, \varepsilon^{\widetilde{\mathcal{F}}} \rceil(\underline{\mathrm{curl}}(\underline{\omega}^*))\|_{(\rho)^{-1}} + \|\lfloor \mu,\, \mathcal{F}^{\widetilde{\mathcal{E}}} \rceil(\underline{\omega})\|_{(\mu)^{-1}} + \|\lfloor \rho,\, \varepsilon^{\widetilde{\mathcal{F}}} \rceil(\underline{u})\|_{(\rho)^{-1}}. \tag{40c}$$

Moreover, if $\underline{u}, \underline{\omega}, \underline{\mathrm{curl}}(\underline{\omega}^*) \in [H^1(\mathrm{C})]^3$ and $\underline{\mathrm{curl}}(\underline{f}) \in [L^4(\Omega)]^3$, the following error bounds hold:

$$\|\mathsf{GRAD}(\boldsymbol{\delta p}^*)\|_\rho \lesssim h_\mathrm{M} \left(\|\underline{\mathrm{curl}}(\underline{\omega}^*)\|_{[H^1(\mathrm{C})]^3} + \|\underline{\mathrm{curl}}\, \underline{f}\|_{[L^4(\Omega)]^3} \right), \tag{41a}$$

$$\|\boldsymbol{\delta\omega}\|_\mu \lesssim h_\mathrm{M} \left(\|\underline{\mathrm{curl}}(\underline{\omega}^*)\|_{[H^1(\mathrm{C})]^3} + \|\underline{\mathrm{curl}}\, \underline{f}\|_{[L^4(\Omega)]^3} + \|\underline{\omega}\|_{[H^1(\mathrm{C})]^3} \right), \tag{41b}$$

$$\|\boldsymbol{\delta u}\|_\rho \lesssim h_\mathrm{M} \left(\|\underline{\mathrm{curl}}(\underline{\omega}^*)\|_{[H^1(\mathrm{C})]^3} + \|\underline{\mathrm{curl}}\, \underline{f}\|_{[L^4(\Omega)]^3} + \|\underline{\omega}\|_{[H^1(\mathrm{C})]^3} + \|\underline{u}\|_{[H^1(\mathrm{C})]^3} \right). \tag{41c}$$

Proof. Since $\mathsf{S}_\mathsf{p}^\mathsf{vb}(\rho, \underline{f}) = \mathsf{S}_\mathsf{d}^\mathsf{vb}(\rho, \underline{f}) + \lfloor \rho,\, \varepsilon^{\widetilde{\mathcal{F}}} \rceil(\underline{f})$, the main difference with the proof of Theorem 3.4 is that the error equation (37a) is to be replaced by

$$\widetilde{\mathsf{CURL}} \cdot \mathsf{H}_\mu^{\mathcal{F}\widetilde{\mathcal{E}}} \cdot \mathsf{CURL}(\boldsymbol{\delta u}) + \mathsf{H}_\rho^{\varepsilon\widetilde{\mathcal{F}}} \cdot \mathsf{GRAD}(\boldsymbol{\delta p}^*) = \widetilde{\mathsf{CURL}}(\lfloor \mu,\, \mathcal{F}^{\widetilde{\mathcal{E}}} \rceil(\underline{\omega})) - \lfloor \rho,\, \varepsilon^{\widetilde{\mathcal{F}}} \rceil(\underline{\mathrm{curl}}(\underline{\omega}^*)).$$

The rest of the proof follows along similar lines, and is skipped for brevity. □

Remark 3.2 (Comparison with Theorem 3.4). When the divergence-free part of the external load (i.e., $\underline{\mathrm{curl}}(\underline{\omega}^*)$) is expected to dominate over the irrotational part (i.e., $\underline{\mathrm{grad}}(p^*)$), using a discrete dual load is more appropriate since the error bounds do not depend on $\underline{\mathrm{curl}}(\underline{\omega}^*)$. Alternatively, when the irrotational part is expected to dominate over the divergence-free part, using a discrete primal load is more appropriate since the error bounds do not depend on $\underline{\mathrm{grad}}(p^*)$.

4 Cell-Based Pressure Schemes

4.1 Discrete systems

Cell-based pressure schemes rely on the 3-field curl formulation (2). Introducing the mass density ρ and the viscosity μ leads to

$$\begin{cases} -\mu^{-1}\underline{\omega}^* + \underline{\mathrm{curl}}(\rho^{-1}\underline{\phi}) = \underline{0}, & \text{in } \Omega, \\ \rho^{-1}\,\underline{\mathrm{curl}}(\underline{\omega}^*) + \underline{\mathrm{grad}}(p^*) = \underline{f}, & \text{in } \Omega, \\ \mathrm{div}(\underline{\phi}) = 0, & \text{in } \Omega, \end{cases} \tag{42}$$

recalling that $\underline{\phi} = \rho\underline{u}$, $\underline{\omega} = \underline{\mathrm{curl}}(\underline{u})$, $\underline{\omega}^* = \mu\underline{\omega}$, and $p^* = \frac{p}{\rho}$. We focus on natural BCs for (42), which are given by

$$\underline{u} \times \underline{\nu}_{\partial\Omega} = \underline{u}_\tau^{\mathrm{bc}}, \quad p^* = p^{\mathrm{bc}}, \qquad \text{on } \partial\Omega, \tag{43}$$

with data $\underline{u}_\tau^{\mathrm{bc}}$ and p^{bc}. A discussion similar to that in Remark 3.1 can be made regarding essential BCs.

In cell-based pressure schemes, the DoFs of the pressure potential, denoted $\mathbf{p}^*$, are located at dual mesh vertices (in one-to-one pairing with primal mesh cells). The DoFs of the mass flux, denoted $\boldsymbol{\phi}$, are located at primal faces, while the DoFs of the viscous stress circulation, denoted $\boldsymbol{\omega}^*$, are located at primal edges. There are two discrete Hodge operators, one related to the (reciprocal of) the mass density ρ and the other to the (reciprocal of) the viscosity μ. The discrete Hodge operator $\mathsf{H}_{\rho^{-1}}^{\mathcal{F}\widetilde{\mathcal{E}}}$ links the discrete velocity and mass flux in the form $\mathbf{u} = \mathsf{H}_{\rho^{-1}}^{\mathcal{F}\widetilde{\mathcal{E}}}(\boldsymbol{\phi}) \in \widetilde{\mathcal{E}}$ (compare with $\underline{u} = \rho^{-1}\underline{\phi}$), while the discrete Hodge operator $\mathsf{H}_{\mu^{-1}}^{\mathcal{E}\widetilde{\mathcal{F}}}$ links the discrete vorticity to the discrete viscous stress circulation in the form $\boldsymbol{\omega} = \mathsf{H}_{\mu^{-1}}^{\mathcal{E}\widetilde{\mathcal{F}}}(\boldsymbol{\omega}^*) \in \widetilde{\mathcal{F}}$ (compare with $\underline{\omega} = \mu^{-1}\underline{\omega}^*$). Both discrete Hodge operators are assumed to satisfy the stability and consistency properties (**A**1) and (**A**2). In what follows, we consider the following discrete norms:

$$\|\boldsymbol{\phi}\|_{\rho^{-1}}^2 := \left[\!\left[\boldsymbol{\phi}, \mathsf{H}_{\rho^{-1}}^{\mathcal{F}\widetilde{\mathcal{E}}}(\boldsymbol{\phi})\right]\!\right]_{\mathcal{F}\widetilde{\mathcal{E}}}, \qquad \|\mathbf{u}\|_{(\rho)}^2 := \left[\!\left[(\mathsf{H}_{\rho^{-1}}^{\mathcal{F}\widetilde{\mathcal{E}}})^{-1}(\mathbf{u}), \mathbf{u}\right]\!\right]_{\mathcal{F}\widetilde{\mathcal{E}}}, \tag{44a}$$

$$\|\boldsymbol{\omega}^*\|_{\mu^{-1}}^2 := \left[\!\left[\boldsymbol{\omega}^*, \mathsf{H}_{\mu^{-1}}^{\mathcal{E}\widetilde{\mathcal{F}}}(\boldsymbol{\omega}^*)\right]\!\right]_{\mathcal{E}\widetilde{\mathcal{F}}}, \qquad \|\boldsymbol{\omega}\|_{(\mu)}^2 := \left[\!\left[(\mathsf{H}_{\mu^{-1}}^{\mathcal{E}\widetilde{\mathcal{F}}})^{-1}(\boldsymbol{\omega}), \boldsymbol{\omega}\right]\!\right]_{\mathcal{E}\widetilde{\mathcal{F}}}, \tag{44b}$$

for all $\boldsymbol{\phi} \in \mathcal{F}$, $\mathbf{u} \in \widetilde{\mathcal{E}}$, $\boldsymbol{\omega}^* \in \mathcal{E}$, and $\boldsymbol{\omega} \in \widetilde{\mathcal{F}}$. Owing to the Cauchy–Schwarz inequality, we infer that

$$\left[\!\left[\boldsymbol{\phi}, \mathbf{u}\right]\!\right]_{\mathcal{F}\widetilde{\mathcal{E}}} \le \|\boldsymbol{\phi}\|_{\rho^{-1}}\,\|\mathbf{u}\|_{(\rho)}, \qquad \left[\!\left[\boldsymbol{\omega}^*, \boldsymbol{\omega}\right]\!\right]_{\mathcal{E}\widetilde{\mathcal{F}}} \le \|\boldsymbol{\omega}^*\|_{\mu^{-1}}\,\|\boldsymbol{\omega}\|_{(\mu)}. \tag{45}$$

We introduce the following operators:

$$\begin{array}{llllll} \mathsf{A}^{\mathsf{cb}} : \mathcal{E} \to \widetilde{\mathcal{F}}, & \mathsf{C} : \mathcal{E} \to \widetilde{\mathcal{E}}, & \mathsf{C}^{\mathrm{T}} : \mathcal{F} \to \widetilde{\mathcal{F}}, & \mathsf{D} : \mathcal{F} \to \mathcal{C}, & \mathsf{D}^{\mathrm{T}} : \widetilde{\mathcal{V}} \to \widetilde{\mathcal{E}}, \\ \mathsf{A}^{\mathsf{cb}} := -\mathsf{H}_{\mu^{-1}}^{\mathcal{E}\widetilde{\mathcal{F}}}, & \mathsf{C} := \mathsf{H}_{\rho^{-1}}^{\mathcal{F}\widetilde{\mathcal{E}}} \cdot \mathsf{CURL}, & \mathsf{C}^{\mathrm{T}} := \widetilde{\mathsf{CURL}} \cdot \mathsf{H}_{\rho^{-1}}^{\mathcal{F}\widetilde{\mathcal{E}}}, & \mathsf{D} := -\mathsf{DIV}, & \mathsf{D}^{\mathrm{T}} := \widetilde{\mathsf{GRAD}}. \end{array} \tag{46}$$

The operators C (resp. D) and C^{T} (resp. D^{T}) are adjoint owing to the adjunction property (13) and the selfadjointness of $\mathsf{H}_{\rho^{-1}}^{\mathcal{F}\widetilde{\mathcal{E}}}$; moreover, A^{cb} is selfadjoint and negative definite.

The cell-based pressure scheme with homogeneous natural BCs is: Find $(\mathbf{p}^*, \boldsymbol{\phi}, \boldsymbol{\omega}^*) \in \widetilde{\mathcal{V}} \times \mathcal{F} \times \mathcal{E}$ such that

$$\begin{pmatrix} \mathsf{A}^{\mathsf{cb}} & \mathsf{C}^{\mathrm{T}} & 0 \\ \mathsf{C} & 0 & \mathsf{D}^{\mathrm{T}} \\ 0 & \mathsf{D} & 0 \end{pmatrix} \begin{pmatrix} \boldsymbol{\omega}^* \\ \boldsymbol{\phi} \\ \mathbf{p}^* \end{pmatrix} = \begin{pmatrix} 0_{\widetilde{\mathcal{F}}} \\ \mathsf{S}^{\mathsf{cb}}(\rho, \underline{f}) \\ 0_{\mathcal{C}} \end{pmatrix} \tag{47}$$

The right-hand side $\mathsf{S}^{\mathsf{cb}}(\rho, \underline{f}) \in \widetilde{\mathcal{E}}$ discretizes the external load $\underline{f}$. Two expressions are considered in the analysis, respectively termed discrete primal and dual load and defined as follows:

$$\mathsf{S}_{\mathsf{p}}^{\mathsf{cb}}(\rho, \underline{f})|_{\tilde{\mathrm{e}}(\mathrm{f})} := \left(\mathsf{H}_{\rho^{-1}}^{\mathcal{F}\widetilde{\mathcal{E}}} \cdot \mathsf{R}_{\mathcal{F}}(\rho\underline{f})\right)|_{\tilde{\mathrm{e}}(\mathrm{f})}, \qquad \mathsf{S}_{\mathsf{d}}^{\mathsf{cb}}(\rho, \underline{f})|_{\tilde{\mathrm{e}}(\mathrm{f})} := \mathsf{R}_{\widetilde{\mathcal{E}}}(\underline{f})|_{\tilde{\mathrm{e}}(\mathrm{f})}, \qquad \forall \mathrm{f} \in \mathrm{F}. \tag{48}$$

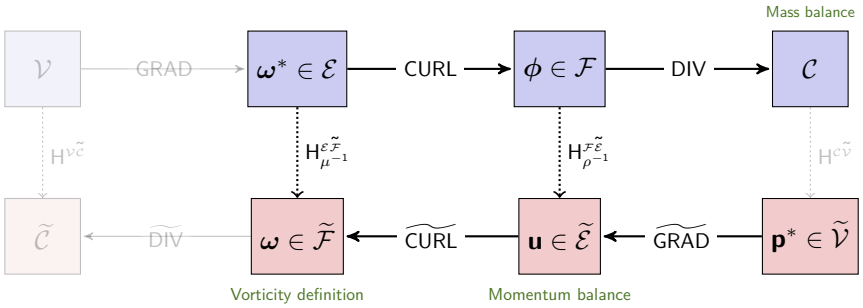

Figure 4: Tonti diagram of the cell-based pressure scheme for the Stokes equations.

Furthermore, non-homogeneous natural BCs can be easily incorporated by modifying the right-hand side of (47) accordingly. We observe that in (47), mass balance holds in each primal cell and momentum balance at each dual edge; moreover, $\boldsymbol{\omega} = \widetilde{\mathsf{CURL}}(\mathbf{u})$ holds. All the relations involved in (47) are summarized in Figure 4.

4.2 Stability and well-posedness

Owing to (**A**1) and recalling (19), the norms $\|\cdot\|_{2,\mathcal{E}}$ and $\|\cdot\|_{\mu^{-1}}$ are uniformly equivalent on $\mathcal{E}$ (with respect to the mesh size); the same holds for the norms $\|\cdot\|_{2,\mathcal{F}}$ and $\|\cdot\|_{\rho^{-1}}$ on $\mathcal{F}$. We equip $\widetilde{\mathcal{V}}$ with the norm $\|\mathbf{p}\|^2_{2,\widetilde{\mathcal{V}}} := \sum_{\mathrm{c}\in\mathrm{C}}|\mathrm{c}|(\mathbf{p}_{\widetilde{\mathrm{v}}(\mathrm{c})})^2$ and $\widetilde{\mathcal{E}}$ with the norm $\|\mathbf{g}\|^2_{2,\widetilde{\mathcal{E}}} := \sum_{\mathrm{c}\in\mathrm{C}}\sum_{\mathrm{f}\in\mathrm{F}_\mathrm{c}}|\mathfrak{p}_{\mathrm{f},\mathrm{c}}|(\frac{\mathbf{g}_{\widetilde{\mathrm{e}}(\mathrm{f})}}{|\widetilde{\mathrm{e}}(\mathrm{f})|})^2$ where $\mathfrak{p}_{\mathrm{f},\mathrm{c}}$ is illustrated in Figure 2. Under assumption ($\mathbf{H}_\mathrm{M}$), the following discrete Poincaré inequality is proved in [9]: There exists $C_\mathrm{P}^{(\delta)}$ such that, for all $\mathbf{p} \in \widetilde{\mathcal{V}}$,

$$\|\mathbf{p}\|_{2,\widetilde{\mathcal{V}}} \le C_\mathrm{P}^{(\delta)} \|\widetilde{\mathsf{GRAD}}(\mathbf{p})\|_{2,\widetilde{\mathcal{E}}}. \tag{49}$$

Lemma 4.1 (Discrete inf-sup conditions)**.** *Assume ($\mathbf{H}_\mathrm{M}$) and ($\mathbf{H}_\mathbf{\Omega}$). Then, there exist $\beta_\mathsf{C} > 0$ and $\beta_\mathsf{D} > 0$ (independent of the mesh size) such that*

$$\inf_{\mathbf{p}\in\widetilde{\mathcal{V}}}\sup_{\mathbf{v}\in\mathcal{F}}\frac{[\![\mathsf{D}(\mathbf{v}),\mathbf{p}]\!]_{\mathcal{C}\widetilde{\mathcal{V}}}}{\|\mathbf{p}\|_{2,\widetilde{\mathcal{V}}}\|\mathbf{v}\|_{\rho^{-1}}} \ge \beta_\mathsf{D}, \qquad \inf_{\boldsymbol{\phi}\in\mathrm{Ker}\,\mathsf{D}}\sup_{\boldsymbol{\psi}\in\mathcal{E}}\frac{[\![\boldsymbol{\phi},\mathsf{C}(\boldsymbol{\psi})]\!]_{\mathcal{F}\widetilde{\mathcal{E}}}}{\|\boldsymbol{\phi}\|_{\rho^{-1}}\|\boldsymbol{\psi}\|_{\mu^{-1}}} \ge \beta_\mathsf{C}.$$

Proof. To prove the inf-sup condition on D, let $\mathbf{p} \in \widetilde{\mathcal{V}}$ and set $\mathbf{v} := (\mathsf{H}^{\mathcal{F}\widetilde{\mathcal{E}}}_{\rho^{-1}})^{-1}(\widetilde{\mathsf{GRAD}}(\mathbf{p}))$. Then, $\mathbf{v} \in \mathcal{F}$, $[\![\mathsf{D}(\mathbf{v}),\mathbf{p}]\!]_{\mathcal{C}\widetilde{\mathcal{V}}} = \|\mathbf{v}\|^2_{\rho^{-1}}$, and $\|\widetilde{\mathsf{GRAD}}(\mathbf{p})\|_{2,\widetilde{\mathcal{E}}} \lesssim \|\mathbf{v}\|_{\rho^{-1}}$ owing to mesh regularity and (**A**1); hence, $\|\mathbf{p}\|_{2,\widetilde{\mathcal{V}}} \lesssim \|\mathbf{v}\|_{\rho^{-1}}$ owing to the discrete Poincaré inequality (49). To prove the inf-sup condition on C, let $\boldsymbol{\phi} \in \mathrm{Ker}\,\mathsf{D}$. Owing to the exact sequence property (7), there is $\boldsymbol{\psi} \in \mathcal{E}$ s.t. $\boldsymbol{\phi} = \mathsf{CURL}(\boldsymbol{\psi})$; moreover, we can take $\boldsymbol{\psi} \in (\mathrm{Ker}\,\mathsf{CURL})^{\perp_\mathsf{H}}$, the orthogonality being with respect to $\mathsf{H}^{\mathcal{E}\widetilde{\mathcal{F}}}_{\mu^{-1}}$. Then, $[\![\boldsymbol{\phi},\mathsf{C}(\boldsymbol{\psi})]\!]_{\mathcal{F}\widetilde{\mathcal{E}}} = \|\boldsymbol{\phi}\|^2_{\rho^{-1}}$ and $\|\boldsymbol{\psi}\|_{2,\mathcal{E}} \lesssim \|\boldsymbol{\phi}\|_{2,\mathcal{F}}$ owing to Lemma 2.2. The norm equivalences on $\mathcal{E}$ and $\mathcal{F}$ conclude the proof. □

A classical consequence of Lemma 4.1 and the fact that A^{cb} is selfadjoint and negative definite is the following [24, Theorem 1]:

Corollary 4.2 (Well-posedness)**.** *Assume ($\mathbf{H}_\mathrm{M}$) and ($\mathbf{H}_\mathbf{\Omega}$). Then, the discrete system* (47) *is well-posed.*

4.3 Error analysis for discrete dual load

Let $(p^*, \underline{\phi}, \underline{\omega}^*)$ solve the 3-field curl formulation (42). Let $(\mathbf{p}^*, \boldsymbol{\phi}, \boldsymbol{\omega}^*)$ solve the discrete system (47). We define the following discrete errors:

$$\boldsymbol{\delta}\mathbf{p}^* := \mathsf{R}_{\widetilde{\mathcal{V}}}(p^*) - \mathbf{p}^*, \quad \boldsymbol{\delta}\boldsymbol{\phi} := \mathsf{R}_\mathcal{F}(\underline{\phi}) - \boldsymbol{\phi}, \quad \boldsymbol{\delta}\boldsymbol{\omega}^* := \mathsf{R}_\mathcal{E}(\underline{\omega}^*) - \boldsymbol{\omega}^*. \tag{50}$$

Recall the global commuting operators $\lfloor \rho^{-1}, {}_{\mathcal{F}}\tilde{\varepsilon}\rceil(\bullet) := \mathsf{H}^{\mathcal{F}\tilde{\varepsilon}}_{\rho^{-1}} \cdot \mathsf{R}_{\mathcal{F}}(\bullet) - \mathsf{R}_{\widetilde{\mathcal{E}}}(\rho^{-1}\bullet)$ and $\lfloor \mu^{-1}, {}_{\mathcal{E}}\tilde{\mathcal{F}}\rceil(\bullet) := \mathsf{H}^{\mathcal{E}\tilde{\mathcal{F}}}_{\mu^{-1}} \cdot \mathsf{R}_{\mathcal{E}}(\bullet) - \mathsf{R}_{\widetilde{\mathcal{F}}}(\mu^{-1}\bullet)$. For simplicity, we assume that there are no quadrature errors when evaluating the external load.

Theorem 4.3 (Error bounds with discrete dual load)**.** *Let $(p^*, \underline{\phi}, \underline{\omega}^*)$ solve the 3-field curl formulation* (42) *with homogeneous natural BCs. Let $(\mathbf{p}^*, \boldsymbol{\phi}, \boldsymbol{\omega}^*)$ solve the discrete system* (47) *with the discrete dual load $\mathsf{S}^{\mathsf{cb}}_{\mathsf{d}}(\rho, \underline{f})$. Assume ($\mathbf{H}_{\mathrm{M}}$) and ($\mathbf{H}_{\boldsymbol{\Omega}}$). Then, the following error bounds hold:*

$$\|\widetilde{\mathsf{GRAD}}(\boldsymbol{\delta}\mathbf{p}^*)\|_{(\rho)} \leq \|\lfloor \rho^{-1}, {}_{\mathcal{F}}\tilde{\varepsilon}\rceil(\underline{\mathrm{curl}}\,\underline{\omega}^*)\|_{(\rho)}, \tag{51a}$$

$$\|\boldsymbol{\delta}\boldsymbol{\omega}^*\|_{\mu^{-1}} \lesssim \|\lfloor \rho^{-1}, {}_{\mathcal{F}}\tilde{\varepsilon}\rceil(\underline{\mathrm{curl}}\,\underline{\omega}^*)\|_{(\rho)} + \|\lfloor \mu^{-1}, {}_{\mathcal{E}}\tilde{\mathcal{F}}\rceil(\underline{\omega}^*)\|_{(\mu)}, \tag{51b}$$

$$\|\boldsymbol{\delta}\boldsymbol{\phi}\|_{\rho^{-1}} \lesssim \|\lfloor \rho^{-1}, {}_{\mathcal{F}}\tilde{\varepsilon}\rceil(\underline{\mathrm{curl}}\,\underline{\omega}^*)\|_{(\rho)} + \|\lfloor \mu^{-1}, {}_{\mathcal{E}}\tilde{\mathcal{F}}\rceil(\underline{\omega}^*)\|_{(\mu)} + \|\lfloor \rho^{-1}, {}_{\mathcal{F}}\tilde{\varepsilon}\rceil(\underline{\phi})\|_{(\rho)}. \tag{51c}$$

Moreover, if $\underline{\omega}^*, \underline{\mathrm{curl}}(\underline{\omega}^*), \underline{\phi} \in [H^1(\mathrm{C})]^3$ and $\underline{\mathrm{curl}}(\underline{f}) \in [L^4(\Omega)]^3$, the following error bounds hold:

$$\|\widetilde{\mathsf{GRAD}}(\boldsymbol{\delta}\mathbf{p}^*)\|_{(\rho)} \lesssim h_{\mathrm{M}} \left(\|\underline{\mathrm{curl}}(\underline{\omega}^*)\|_{[H^1(\mathrm{C})]^3} + \|\underline{\mathrm{curl}}(\underline{f})\|_{[L^4(\Omega)]^3} \right), \tag{52a}$$

$$\|\boldsymbol{\delta}\boldsymbol{\omega}^*\|_{\mu^{-1}} \lesssim h_{\mathrm{M}} \left(\|\underline{\mathrm{curl}}(\underline{\omega}^*)\|_{[H^1(\mathrm{C})]^3} + \|\underline{\mathrm{curl}}(\underline{f})\|_{[L^4(\Omega)]^3} + \|\underline{\omega}^*\|_{[H^1(\mathrm{C})]^3} \right), \tag{52b}$$

$$\|\boldsymbol{\delta}\boldsymbol{\phi}\|_{\rho^{-1}} \lesssim h_{\mathrm{M}} \left(\|\underline{\mathrm{curl}}(\underline{\omega}^*)\|_{[H^1(\mathrm{C})]^3} + \|\underline{\mathrm{curl}}(\underline{f})\|_{[L^4(\Omega)]^3} + \|\underline{\omega}^*\|_{[H^1(\mathrm{C})]^3} + \|\underline{\phi}\|_{[H^1(\mathrm{C})]^3} \right). \tag{52c}$$

Proof. (1) We first derive the error equations. Applying $\mathsf{R}_{\widetilde{\mathcal{F}}}$ to the vorticity definition, $\mathsf{R}_{\widetilde{\mathcal{E}}}$ to the momentum balance, and $\mathsf{R}_{\mathcal{C}}$ to the mass balance in (42) yields

$$\begin{aligned} -\mathsf{R}_{\widetilde{\mathcal{F}}}(\mu^{-1}\underline{\omega}^*) + \widetilde{\mathsf{CURL}}(\mathsf{R}_{\widetilde{\mathcal{E}}}(\rho^{-1}\underline{\phi})) &= 0_{\widetilde{\mathcal{F}}}, \\ \mathsf{R}_{\widetilde{\mathcal{E}}}(\rho^{-1}\,\underline{\mathrm{curl}}(\underline{\omega}^*)) + \widetilde{\mathsf{GRAD}}(\mathsf{R}_{\widetilde{\mathcal{V}}}(p^*)) &= \mathsf{S}^{\mathsf{cb}}_{\mathsf{d}}(\rho, \underline{f}), \\ \mathsf{DIV}(\mathsf{R}_{\mathcal{F}}(\underline{\phi})) &= 0_{\mathcal{C}}, \end{aligned}$$

owing to the commuting property 9 on the interior dual mesh entities and the homogeneous BCs (43) on the dual mesh entities touching the boundary $\partial\Omega$. Subtracting from the corresponding equation in (47) and introducing the global commuting operators leads to

$$-\mathsf{H}^{\mathcal{E}\tilde{\mathcal{F}}}_{\mu^{-1}}(\boldsymbol{\delta}\boldsymbol{\omega}^*) + \widetilde{\mathsf{CURL}} \cdot \mathsf{H}^{\mathcal{F}\tilde{\mathcal{E}}}_{\rho^{-1}}(\boldsymbol{\delta}\boldsymbol{\phi}) = -\lfloor \mu^{-1}, {}_{\mathcal{E}}\tilde{\mathcal{F}}\rceil(\underline{\omega}^*) + \widetilde{\mathsf{CURL}} \cdot \lfloor \rho^{-1}, {}_{\mathcal{F}}\tilde{\varepsilon}\rceil(\underline{\phi}), \tag{53a}$$

$$\mathsf{H}^{\mathcal{F}\tilde{\mathcal{E}}}_{\rho^{-1}} \cdot \mathsf{CURL}(\boldsymbol{\delta}\boldsymbol{\omega}^*) + \widetilde{\mathsf{GRAD}}(\boldsymbol{\delta}\mathbf{p}^*) = \lfloor \rho^{-1}, {}_{\mathcal{F}}\tilde{\varepsilon}\rceil(\underline{\mathrm{curl}}\,\underline{\omega}^*), \tag{53b}$$

$$\mathsf{DIV}(\boldsymbol{\delta}\boldsymbol{\phi}) = 0_{\mathcal{C}}. \tag{53c}$$

(2) Bound on the pressure gradient. We take the duality product of (53b) with $(\mathsf{H}^{\mathcal{F}\tilde{\mathcal{E}}}_{\rho^{-1}})^{-1} \cdot \widetilde{\mathsf{GRAD}}(\boldsymbol{\delta}\mathbf{p}^*)$. Proceeding as in Step (2) of the proof of Theorem 3.4 yields (51a).
(3) Bound on the viscous stress circulation. We use the discrete Hodge decomposition (38) based on the discrete Hodge operator $\mathsf{H}^{\mathcal{E}\tilde{\mathcal{F}}}_{\mu^{-1}}$. We set $\boldsymbol{\delta}\boldsymbol{\omega}^* = \mathsf{GRAD}(\boldsymbol{\delta}\boldsymbol{\theta}) + \boldsymbol{\delta}\boldsymbol{\omega}^*_{\perp}$ with $\boldsymbol{\delta}\boldsymbol{\theta} \in \mathcal{V}$ and $\boldsymbol{\delta}\boldsymbol{\omega}^*_{\perp} \in (\mathrm{Ker}\,\mathsf{CURL})^{\perp_{\mathsf{H}}}$. We take the duality product of (53a) with $\mathsf{GRAD}(\boldsymbol{\delta}\boldsymbol{\theta})$. Observing that $\big[\!\big[\mathsf{GRAD}(\boldsymbol{\delta}\boldsymbol{\theta}), \widetilde{\mathsf{CURL}}(\mathbf{x})\big]\!\big]_{\mathcal{E}\tilde{\mathcal{F}}} = 0$ for all $\mathbf{x} \in \widetilde{\mathcal{E}}$ and $\big[\!\big[\mathsf{GRAD}(\boldsymbol{\delta}\boldsymbol{\theta}), \mathsf{H}^{\mathcal{E}\tilde{\mathcal{F}}}_{\mu^{-1}}(\boldsymbol{\delta}\boldsymbol{\omega}^*)\big]\!\big]_{\mathcal{E}\tilde{\mathcal{F}}} = \|\mathsf{GRAD}(\boldsymbol{\theta})\|^2_{\mu^{-1}}$, we infer that $\|\mathsf{GRAD}(\boldsymbol{\theta})\|_{\mu^{-1}} \lesssim \|\lfloor \mu^{-1}, {}_{\mathcal{E}}\tilde{\mathcal{F}}\rceil(\underline{\omega}^*)\|_{(\mu)}$. Then, we take the duality product of (53b) with $\mathsf{CURL}(\boldsymbol{\delta}\boldsymbol{\omega}^*)$. This yields $\|\mathsf{CURL}(\boldsymbol{\delta}\boldsymbol{\omega}^*)\|_{\rho^{-1}} \leq \|\lfloor \rho^{-1}, {}_{\mathcal{F}}\tilde{\varepsilon}\rceil(\underline{\mathrm{curl}}\,\underline{\omega}^*)\|_{(\rho)}$. Since $\mathsf{CURL}(\boldsymbol{\delta}\boldsymbol{\omega}^*) = \mathsf{CURL}(\boldsymbol{\delta}\boldsymbol{\omega}^*_{\perp})$ and $\boldsymbol{\delta}\boldsymbol{\omega}^*_{\perp} \in (\mathrm{Ker}\,\mathsf{CURL})^{\perp_{\mathsf{H}}}$, we infer from Lemma 2.2 that

$$\|\boldsymbol{\delta}\boldsymbol{\omega}^*_{\perp}\|_{\mu^{-1}} \lesssim \|\lfloor \rho^{-1}, {}_{\mathcal{F}}\tilde{\varepsilon}\rceil(\underline{\mathrm{curl}}\,\underline{\omega}^*)\|_{(\rho)}.$$

Finally, since $\|\boldsymbol{\delta}\boldsymbol{\omega}^*\|^2_{\mu^{-1}} = \|\mathsf{GRAD}(\boldsymbol{\theta})\|^2_{\mu^{-1}} + \|\boldsymbol{\delta}\boldsymbol{\omega}^*_{\perp}\|^2_{\mu^{-1}}$, we infer (51b).
(4) Bound on the mass flux. Owing to (53c), ($\mathbf{H}_{\boldsymbol{\Omega}}$), and (7), there is $\boldsymbol{\delta}\boldsymbol{\psi} \in \mathcal{E}$ s.t. $\boldsymbol{\delta}\boldsymbol{\phi} = \mathsf{CURL}(\boldsymbol{\delta}\boldsymbol{\psi})$, and we can take $\boldsymbol{\delta}\boldsymbol{\psi} \in (\mathrm{Ker}\,\mathsf{CURL})^{\perp_{\mathsf{H}}}$. We take the duality product of (53a) with $\boldsymbol{\delta}\boldsymbol{\psi}$. For the two terms on the left-hand side, we obtain $\big[\!\big[\boldsymbol{\delta}\boldsymbol{\psi}, \mathsf{H}^{\mathcal{E}\tilde{\mathcal{F}}}_{\mu^{-1}}(\boldsymbol{\delta}\boldsymbol{\omega}^*)\big]\!\big]_{\mathcal{E}\tilde{\mathcal{F}}} \leq \|\boldsymbol{\delta}\boldsymbol{\psi}\|_{\mu^{-1}}\|\boldsymbol{\delta}\boldsymbol{\omega}^*\|_{\mu^{-1}}$ and $\big[\!\big[\boldsymbol{\delta}\boldsymbol{\psi}, \widetilde{\mathsf{CURL}} \cdot \mathsf{H}^{\mathcal{F}\tilde{\mathcal{E}}}_{\rho^{-1}}(\boldsymbol{\delta}\boldsymbol{\phi})\big]\!\big]_{\mathcal{E}\tilde{\mathcal{F}}} = \|\mathsf{CURL}(\boldsymbol{\delta}\boldsymbol{\psi})\|^2_{\rho^{-1}}$. Using Lemma 2.2, Cauchy–Schwarz inequalities, and the previous error bounds leads to (51c).
(5) Finally, the error bounds for smooth solutions result from Lemma 2.3. □

4.4 Error analysis for discrete primal load

Theorem 4.4 (Error bounds with discrete primal load)**.** *Let $(p^*, \underline{\phi}, \underline{\omega}^*)$ solve the 3-field curl formulation* (42) *with homogeneous natural BCs. Let $(\mathbf{p}^*, \boldsymbol{\phi}, \boldsymbol{\omega}^*)$ solve the discrete system* (47) *with the discrete primal load $\mathsf{S}_{\mathsf{p}}^{\mathsf{cb}}(\rho, \underline{f})$. Assume (**H**$_{\mathrm{M}}$) and (**H**$_{\boldsymbol{\Omega}}$). Then, the following error bounds hold:*

$$\|\widetilde{\mathsf{GRAD}}(\boldsymbol{\delta}\mathbf{p}^*)\|_{(\rho)} \le \|\lfloor\rho^{-1}, \tilde{\varepsilon}\rceil(\rho\,\underline{\mathrm{grad}}(p^*)\|_{(\rho)}, \tag{54a}$$

$$\|\boldsymbol{\delta\omega}^*\|_{\mu^{-1}} \lesssim \|\lfloor\rho^{-1}, \tilde{\varepsilon}\rceil(\rho\,\underline{\mathrm{grad}}(p^*))\|_{(\rho)} + \|\lfloor\mu^{-1}, \tilde{\varepsilon}\rceil(\underline{\omega}^*)\|_{(\mu)}, \tag{54b}$$

$$\|\boldsymbol{\delta\phi}\|_{\rho^{-1}} \lesssim \|\lfloor\rho^{-1}, \tilde{\varepsilon}\rceil(\rho\,\underline{\mathrm{grad}}(p^*))\|_{(\rho)} + \|\lfloor\mu^{-1}, \tilde{\varepsilon}\rceil(\underline{\omega}^*)\|_{(\mu)} + \|\lfloor\rho^{-1}, \tilde{\varepsilon}\rceil(\underline{\phi})\|_{(\rho)}. \tag{54c}$$

Moreover, if $\underline{\omega}^*, \underline{\phi}, \underline{\mathrm{grad}}(p^*) \in [H^1(\mathrm{C})]^3$ and $\underline{f} \in [L^4(\Omega)]^3$, the following error bounds hold:

$$\|\widetilde{\mathsf{GRAD}}(\boldsymbol{\delta}\mathbf{p}^*)\|_{(\rho)} \lesssim h_{\mathrm{M}}\,\|\rho\,\underline{\mathrm{grad}}(p^*)\|_{[H^1(\mathrm{C})]^3}, \tag{55a}$$

$$\|\boldsymbol{\delta\omega}^*\|_{\mu^{-1}} \lesssim h_{\mathrm{M}}\left(\|\rho\,\underline{\mathrm{grad}}(p^*)\|_{[H^1(\mathrm{C})]^3} + \|\underline{\omega}^*\|_{[H^1(\mathrm{C})]^3} + \|\underline{f}\|_{[L^4(\Omega)]^3}\right), \tag{55b}$$

$$\|\boldsymbol{\delta\phi}\|_{\rho^{-1}} \lesssim h_{\mathrm{M}}\left(\|\rho\,\underline{\mathrm{grad}}(p^*)\|_{[H^1(\mathrm{C})]^3} + \|\underline{\omega}^*\|_{[H^1(\mathrm{C})]^3} + \|\underline{f}\|_{[L^4(\Omega)]^3} + \|\underline{\phi}\|_{[H^1(\mathrm{C})]^3}\right). \tag{55c}$$

Proof. Since $\mathsf{S}_{\mathsf{p}}^{\mathsf{cb}}(\rho, \underline{f}) = \mathsf{S}_{\mathsf{d}}^{\mathsf{cb}}(\rho, \underline{f}) + \lfloor\rho^{-1}, \tilde{\varepsilon}\rceil(\rho\underline{f})$, the main difference with the proof of Theorem 4.3 is that the error equation (53b) is to be replaced by

$$\mathsf{H}_{\rho^{-1}}^{\tilde{\varepsilon}} \cdot \mathsf{CURL}(\boldsymbol{\delta\omega}^*) + \widetilde{\mathsf{GRAD}}(\boldsymbol{\delta}\mathbf{p}^*) = \lfloor\rho^{-1}, \tilde{\varepsilon}\rceil(\rho\,\underline{\mathrm{grad}}(p^*)).$$

The rest of the proof follows along similar lines, and is skipped for brevity. □

Remark 4.1 (Comparison with Theorem 4.3). When the divergence-free part of the external load (i.e., $\underline{\mathrm{curl}}(\underline{\omega}^*)$) is expected to dominate over the irrotational part (i.e., $\underline{\mathrm{grad}}(p^*)$), using a discrete primal load is more appropriate since the error bounds do not depend on $\underline{\mathrm{curl}}(\underline{\omega}^*)$. Alternatively, when the irrotational part is expected to dominate over the divergence-free part, using a discrete dual load is more appropriate since the error bounds do not depend on $\underline{\mathrm{grad}}(p^*)$.

5 Numerical Results

We investigate numerically the vertex-based pressure schemes of Section 3 in the case of natural and essential BCs, and for both primal and dual discretizations of the external load. We consider the four combinations: natural (Nat.) BCs & $\mathsf{S}_{\mathsf{p}}^{\mathsf{vb}}(\rho, \underline{f})$, essential (Ess.) BCs & $\mathsf{S}_{\mathsf{p}}^{\mathsf{vb}}(\rho, \underline{f})$, Nat. BCs & $\mathsf{S}_{\mathsf{d}}^{\mathsf{vb}}(\rho, \underline{f})$, and Ess. BCs & $\mathsf{S}_{\mathsf{d}}^{\mathsf{vb}}(\rho, \underline{f})$. The two discrete Hodge operators $\mathsf{H}_{\rho}^{\varepsilon\tilde{\mathcal{F}}}$ and $\mathsf{H}_{\mu}^{\mathcal{F}\tilde{\varepsilon}}$ are built using the DGA reconstruction functions; see [17]. The resulting discrete Hodge operators satisfy the stability and $\mathbb{P}_0$-consistency properties (**A**1) and (**A**2); see [9]. We consider the system (24) on the unit cube $\Omega = [0,1]^3$ with mass density and viscosity set to 1. The exact pressure and velocity are

$$p(x,y,z) = \sin(2\pi x)\sin(2\pi y)\sin(2\pi z), \qquad \underline{u}(x,y,z) = \begin{bmatrix} \frac{1}{2}\sin(2\pi x)\cos(2\pi y)\cos(2\pi z) \\ \frac{1}{2}\cos(2\pi x)\sin(2\pi y)\cos(2\pi z) \\ -\cos(2\pi x)\cos(2\pi y)\sin(2\pi z) \end{bmatrix}. \tag{56}$$

The external load $\underline{f}$ and the BCs are determined from (56). Two sequences of three-dimensional polyhedral meshes of the FVCA6 benchmark [see 26] are tested. The first mesh sequence, labeled PrG, contains prismatic meshes with polygonal basis, and the second sequence, labeled CB, checkerboard meshes, the latter being a classical example of so-called non-matching meshes. Each mesh family consists of successive uniform refinements of an initial mesh. Examples are shown in Figure 5 and quantitative information on the meshes is provided in Table 1.

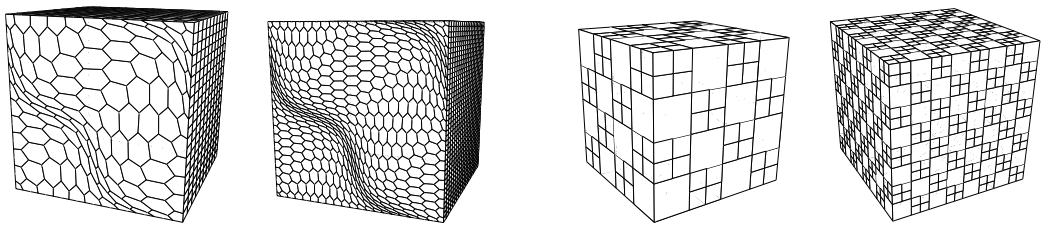

Figure 5: Two examples of prismatic meshes with polygonal basis (left) and of checkerboard meshes (right).

Sequence	Mesh	#V	#E	#F	#C
PrG	coarsest	3 080	7 200	5 331	1 210
	finest	144 320	354 000	276 921	67 240
CB	coarsest	625	1 536	1 200	288
	finest	254 977	700 416	592 896	147 456

Table 1: Cardinality of the mesh entity sets for the coarsest and finest meshes of the PrG and CB mesh sequences

To study the convergence rate of the CDO schemes, we report the following errors:

$$\begin{aligned} \mathrm{Er}_{\mathsf{H}_1}(\mathbf{p}) &:= \frac{\|\mathsf{R}_{\mathcal{V}}(p^*) - \mathbf{p}^*\|_1}{\|\mathsf{R}_{\mathcal{V}}(p^*)\|_1}, \qquad \mathrm{Er}_{\mathsf{H}\rho}(\mathbf{g}) := \frac{\|\mathsf{R}_{\mathcal{E}}(\underline{\mathrm{grad}}(p^*)) - \mathsf{GRAD}(\mathbf{p}^*)\|_\rho}{\|\mathsf{R}_{\mathcal{E}}(\underline{\mathrm{grad}}(p^*))\|_\rho}, \\ \mathrm{Er}_{\mathsf{H}\rho}(\mathbf{u}) &:= \frac{\|\mathsf{R}_{\mathcal{E}}(\underline{u}) - \mathbf{u}\|_\rho}{\|\mathsf{R}_{\mathcal{E}}(\underline{u})\|_\rho}, \qquad \mathrm{Er}_{\mathsf{H}\mu}(\boldsymbol{\omega}) := \frac{\|\mathsf{R}_{\mathcal{E}}(\underline{\mathrm{curl}}\,\underline{u}) - \mathsf{CURL}(\mathbf{u})\|_\mu}{\|\mathsf{R}_{\mathcal{F}}(\underline{\mathrm{curl}}\,\underline{u})\|_\mu}. \end{aligned} \tag{57}$$

The discrete norms $\|\cdot\|_\rho$ and $\|\cdot\|_\mu$ are defined in (27), while $\|\mathbf{a}\|_1^2 := \big[\mathbf{a}, \mathsf{H}_1^{\mathcal{V}\tilde{\mathcal{C}}}(\mathbf{a})\big]_{\mathcal{V}\tilde{\mathcal{C}}} = \|\mathbf{a}\|_{2,\mathcal{V}}^2$, for all $\mathbf{a} \in \mathcal{V}$, with $\mathsf{H}_1^{\mathcal{V}\tilde{\mathcal{C}}}$ defined above Lemma 2.1. Along with the errors defined in (57), we report the observed convergence rates. The convergence rate R between mesh i and mesh $(i-1)$ within a sequence is defined as

$$\mathrm{R} := -3\frac{\log\left(\mathrm{Er}(i)/\mathrm{Er}(i-1)\right)}{\log\left(\#\mathrm{X}(i)/\#\mathrm{X}(i-1)\right)},$$

where #X is equal to #V for the pressure, #E for the pressure gradient and the velocity, and #F for the vorticity. The various errors are plotted in Figure 6 as the meshes are refined and for the four combinations of BCs and load discretization. Convergence rates observed on the finest meshes are reported in Table 2. The results on the pressure gradient, vorticity, and velocity are in accordance with the theoretical results derived in Section 3. In some cases, some super-convergent behavior is observed. The pressure error appears to converge at second-order for most of the cases considered herein.

6 Conclusions

In this work, we have analyzed CDO schemes for the Stokes equations on three-dimensional polyhedral meshes. The distinction between primal and dual meshes enabled us to devise vertex-based and cell-based pressure schemes. Vertex-based pressure schemes lead to an algebraic system of size (#V + #E) with two unknowns, the pressure located at primal vertices and the velocity at primal edges. Cell-based pressure schemes lead to a system of size (#E + #F + #C) with three unknowns, the pressure located at primal cells, the mass flux at primal faces, and the viscous stress circulation at primal edges. For

			$\mathrm{Er}_{\mathsf{H}_1}(\mathbf{p})$	$\mathrm{Er}_{\mathsf{H}\rho}(\mathbf{g})$	$\mathrm{Er}_{\mathsf{H}\rho}(\mathbf{u})$	$\mathrm{Er}_{\mathsf{H}\mu}(\boldsymbol{\omega})$
PrG	Nat. BCs	$\mathsf{S}_\mathsf{p}^{\mathsf{vb}}$	1.7	1.7	1.8	1.7
		$\mathsf{S}_\mathsf{d}^{\mathsf{vb}}$	2.1	1.9	1.8	1.7
	Ess. BCs	$\mathsf{S}_\mathsf{p}^{\mathsf{vb}}$	2.1	1.9	2.0	1.9
		$\mathsf{S}_\mathsf{d}^{\mathsf{vb}}$	2.1	2.0	2.0	1.9
CB	Nat. BCs	$\mathsf{S}_\mathsf{p}^{\mathsf{vb}}$	1.8	1.0	1.1	1.0
		$\mathsf{S}_\mathsf{d}^{\mathsf{vb}}$	2.2	1.1	1.1	1.0
	Ess. BCs	$\mathsf{S}_\mathsf{p}^{\mathsf{vb}}$	1.9	1.1	1.0	1.0
		$\mathsf{S}_\mathsf{d}^{\mathsf{vb}}$	2.0	1.1	1.0	0.9

Table 2: Convergence rates between the two finest meshes of each sequence

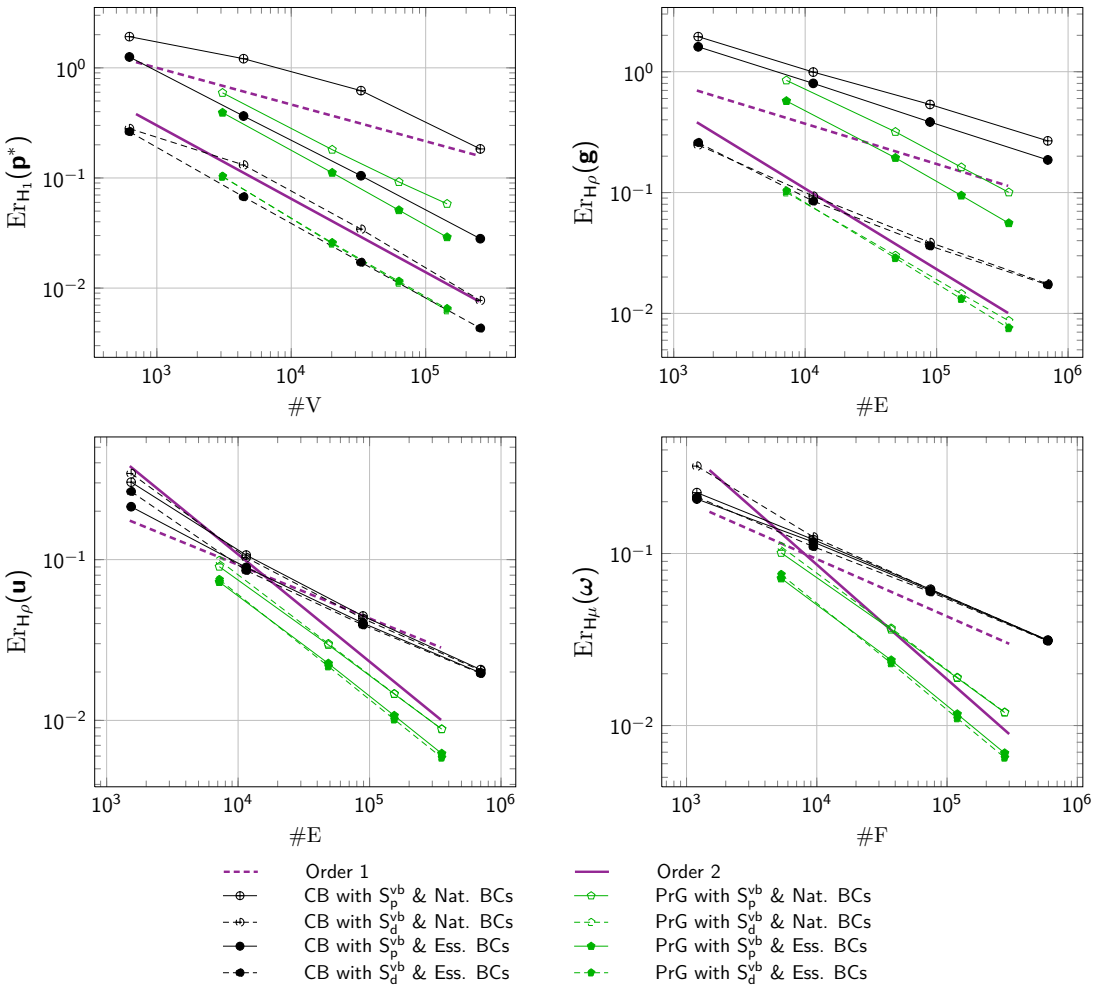

Figure 6: Errors for the two mesh sequences and the four combinations of BCs and load discretization

both schemes, two discrete Hodge operators, related to the mass density and the viscosity, are used; as for elliptic problems, these operators must satisfy a stability and a consistency property. Both schemes conserve mass and momentum, the vertex-based ones at dual cells and dual faces, respectively, and the cell-based ones at primal cells and dual edges, respectively. Finally, both schemes can be deployed with

two possible load discretizations, so as to handle a large irrotational or divergence-free part of the load. Finally, various tracks are worth pursuing in future work, including the use of hybridization techniques for saddle-point problems and the treatment of essential (and more general) BCs as well as complex topologies for the domain Ω.

A Proof of discrete Poincaré inequalities

The proof of the discrete Poincaré inequalities hinges on the existence of conforming reconstruction operators $\mathsf{L}_{\mathcal{V}}^{\rm conf}:\mathcal{V}\to H^1(\Omega)$, $\underline{\mathsf{L}}_{\mathcal{E}}^{\rm conf}:\mathcal{E}\to H(\underline{\rm curl};\Omega)$, and $\underline{\mathsf{L}}_{\mathcal{F}}^{\rm conf}:\mathcal{F}\to H({\rm div};\Omega)$ with right inverse properties $\mathsf{R}_{\mathcal{V}}\mathsf{L}_{\mathcal{V}}^{\rm conf}=\mathsf{Id}_{\mathcal{V}}$, $\mathsf{R}_{\mathcal{E}}\mathsf{L}_{\mathcal{E}}^{\rm conf}=\mathsf{Id}_{\mathcal{E}}$, commuting properties $\underline{\rm grad}(\mathsf{L}_{\mathcal{V}}^{\rm conf})=\underline{\mathsf{L}}_{\mathcal{E}}^{\rm conf}(\mathsf{GRAD})$, $\underline{\rm curl}(\underline{\mathsf{L}}_{\mathcal{E}}^{\rm conf})=\underline{\mathsf{L}}_{\mathcal{F}}^{\rm conf}(\mathsf{CURL})$, and stability properties $C_{\mathcal{V}}^{\flat}\|\mathbf{p}\|_{2,\mathcal{V}}\le\|\mathsf{L}_{\mathcal{V}}^{\rm conf}(\mathbf{p})\|_{L^2(\Omega)}$, $\|\mathsf{L}_{\mathcal{E}}^{\rm conf}(\mathbf{u})\|_{L^2(\Omega)^3}\le C_{\mathcal{E}}^{\sharp}\|\mathbf{u}\|_{2,\mathcal{E}}$, and $\|\mathsf{L}_{\mathcal{F}}^{\rm conf}(\boldsymbol{\phi})\|_{L^2(\Omega)^3}\le C_{\mathcal{F}}^{\sharp}\|\boldsymbol{\phi}\|_{2,\mathcal{F}}$. One possibility is to use the construction of [15] hinging on local constrained minimization problems using Withney finite elements on the simplicial submesh of each mesh cell. Note that the resulting reconstruction operators are polynomial-valued.

Proof of discrete Poincaré–Wirtinger inequality. Let $\mathbf{p}\in\mathcal{V}$ be such that $\big[\mathbf{p},\mathsf{H}_1^{\mathcal{V}\tilde{\mathcal{C}}}(\mathbf{1})\big]_{\mathcal{V}\tilde{\mathcal{C}}}=0$. Set $z:=\mathsf{L}_{\mathcal{V}}^{\rm conf}(\mathbf{p})-\langle\mathsf{L}_{\mathcal{V}}^{\rm conf}(\mathbf{p})\rangle_\Omega\in H^1(\Omega)$ where $\langle\cdot\rangle_\Omega$ denotes the mean-value in Ω. Owing to the continuous Poincaré–Wirtinger inequality, $\|z\|_{L^2(\Omega)}\le C_{\rm P,\Omega}^{(0)}\|\underline{\rm grad}\,z\|_{L^2(\Omega)^3}$. Moreover, owing to the properties of $\mathsf{L}_{\mathcal{V}}^{\rm conf}$ and $\underline{\mathsf{L}}_{\mathcal{E}}^{\rm conf}$, we infer that

$$\|\underline{\rm grad}\,z\|_{L^2(\Omega)^3}=\|\underline{\rm grad}(\mathsf{L}_{\mathcal{V}}^{\rm conf}(\mathbf{p}))\|_{L^2(\Omega)^3}=\|\underline{\mathsf{L}}_{\mathcal{E}}^{\rm conf}(\mathsf{GRAD}(\mathbf{p}))\|_{L^2(\Omega)^3}\le C_{\mathcal{E}}^{\sharp}\|\mathsf{GRAD}(\mathbf{p})\|_{2,\mathcal{E}},$$

so that $\|z\|_{L^2(\Omega)}\le C_{\rm P,\Omega}^{(0)}C_{\mathcal{E}}^{\sharp}\|\mathsf{GRAD}(\mathbf{p})\|_{2,\mathcal{E}}$. Furthermore, since $\mathbf{p}-\mathsf{R}_{\mathcal{V}}(z)=\langle\mathsf{L}_{\mathcal{V}}^{\rm conf}(\mathbf{p})\rangle_\Omega\mathbf{1}$, we infer that

$$\|\mathbf{p}\|_{2,\mathcal{V}}^2=\big[\mathbf{p},\mathsf{H}_1^{\mathcal{V}\tilde{\mathcal{C}}}(\mathbf{p})\big]_{\mathcal{V}\tilde{\mathcal{C}}}=\big[\mathbf{p},\mathsf{H}_1^{\mathcal{V}\tilde{\mathcal{C}}}(\mathbf{p}-\mathsf{R}_{\mathcal{V}}(z))\big]_{\mathcal{V}\tilde{\mathcal{C}}}+\big[\mathbf{p},\mathsf{H}_1^{\mathcal{V}\tilde{\mathcal{C}}}\mathsf{R}_{\mathcal{V}}(z)\big]_{\mathcal{V}\tilde{\mathcal{C}}}=\big[\mathbf{p},\mathsf{H}_1^{\mathcal{V}\tilde{\mathcal{C}}}\mathsf{R}_{\mathcal{V}}(z)\big]_{\mathcal{V}\tilde{\mathcal{C}}},$$

so that $\|\mathbf{p}\|_{2,\mathcal{V}}\le\|\mathsf{R}_{\mathcal{V}}(z)\|_{2,\mathcal{V}}$. Finally, since $\|\mathsf{R}_{\mathcal{V}}(z)\|_{2,\mathcal{V}}\le(C_{\mathcal{V}}^{\flat})^{-1}\|\mathsf{L}_{\mathcal{V}}^{\rm conf}(\mathsf{R}_{\mathcal{V}}(z))\|_{L^2(\Omega)}$ and $\mathsf{L}_{\mathcal{V}}^{\rm conf}(\mathsf{R}_{\mathcal{V}}(z))=z$ (observe in particular that $\mathsf{R}_{\mathcal{V}}(1)=\mathbf{1}$ and $\mathsf{L}_{\mathcal{V}}^{\rm conf}(\mathbf{1})=1$), we infer (20) with $C_{\rm P}^{(0)}=C_{\rm P,\Omega}^{(0)}C_{\mathcal{E}}^{\sharp}(C_{\mathcal{V}}^{\flat})^{-1}$. □

Proof of discrete Poincaré inequality for the curl. Let $\mathbf{u}\in\mathcal{E}$ be such that $\big[\mathbf{u},\mathsf{H}_\alpha^{\mathcal{E}\tilde{\mathcal{F}}}(\mathbf{v})\big]_{\mathcal{E}\tilde{\mathcal{F}}}=0$ for all $\mathbf{v}\in\operatorname{Ker}\mathsf{CURL}$. There is $\underline{z}\in H(\underline{\rm curl};\Omega)$ such that $\underline{\rm curl}(\underline{z})=\underline{\rm curl}(\underline{\mathsf{L}}_{\mathcal{E}}^{\rm conf}(\mathbf{u}))$ and ${\rm div}(\underline{z})=0$ in Ω and $\underline{z}\cdot\underline{\nu}_{\partial\Omega}=0$. For all $\underline{v}\in\operatorname{Ker}(\underline{\rm curl})$, there is $\vartheta\in H^1(\Omega)$ s.t. $\underline{v}=\underline{\rm grad}(\vartheta)$ owing to $(\mathbf{H}_{\boldsymbol{\Omega}})$, so that $\int_\Omega\underline{z}\cdot\underline{v}=\int_\Omega{\rm div}(\underline{z})\vartheta+\int_{\partial\Omega}(\underline{z}\cdot\underline{\nu}_{\partial\Omega})\vartheta=0$. Owing to the continuous Poincaré inequality for the curl, $\|\underline{z}\|_{L^2(\Omega)^3}\le C_{\rm P,\Omega}^{(1)}\|\underline{\rm curl}(\underline{z})\|_{L^2(\Omega)^3}$. Moreover, owing to [2, Prop. 3.7], there is $s>\frac12$ such that $\|\underline{z}\|_{H^s(\Omega)^3}\le C_{H^s}C_{\rm P,\Omega}^{(1)}\|\underline{\rm curl}(\underline{z})\|_{L^2(\Omega)^3}$. This bound implies that $\underline{z}$ is in the domain of the Nédélec finite element interpolation operator on the simplicial submesh, so that, using mesh regularity, the proof of Prop. 4.6 in the above reference, and the fact that $\underline{\rm curl}(\underline{z})$ is polynomial-valued, we infer that $\|\mathsf{R}_{\mathcal{E}}(\underline{z})\|_{2,\mathcal{E}}\le C_{\rm N}C_{H^s}C_{\rm P,\Omega}^{(1)}\|\underline{\rm curl}(\underline{z})\|_{L^2(\Omega)^3}$. Furthermore, we observe that

$$\big[\mathbf{u},\mathsf{H}_\alpha^{\mathcal{E}\tilde{\mathcal{F}}}(\mathbf{u})\big]_{\mathcal{E}\tilde{\mathcal{F}}}=\big[\mathbf{u},\mathsf{H}_\alpha^{\mathcal{E}\tilde{\mathcal{F}}}(\mathbf{u}-\mathsf{R}_{\mathcal{E}}(\underline{z}))\big]_{\mathcal{E}\tilde{\mathcal{F}}}+\big[\mathbf{u},\mathsf{H}_\alpha^{\mathcal{E}\tilde{\mathcal{F}}}(\mathsf{R}_{\mathcal{E}}(\underline{z}))\big]_{\mathcal{E}\tilde{\mathcal{F}}}=\big[\mathbf{u},\mathsf{H}_\alpha^{\mathcal{E}\tilde{\mathcal{F}}}(\mathsf{R}_{\mathcal{E}}(\underline{z}))\big]_{\mathcal{E}\tilde{\mathcal{F}}},$$

since

$$\mathsf{CURL}(\mathbf{u}-\mathsf{R}_{\mathcal{E}}(\underline{z}))=\mathsf{CURL}(\mathsf{R}_{\mathcal{E}}(\underline{\mathsf{L}}_{\mathcal{E}}^{\rm conf}(\mathbf{u})-\underline{z}))=\mathsf{R}_{\mathcal{F}}(\underline{\rm curl}(\underline{\mathsf{L}}_{\mathcal{E}}^{\rm conf}(\mathbf{u})-\underline{z}))=0.$$

Hence, $\|\mathbf{u}\|_\alpha\le\|\mathsf{R}_{\mathcal{E}}(\underline{z})\|_\alpha$, and owing to $(\mathbf{A}1)$, we infer that

$$\eta_\alpha\|\mathbf{u}\|_{2,\mathcal{E}}\le\|\mathsf{R}_{\mathcal{E}}(\underline{z})\|_{2,\mathcal{E}}\le C_{\rm N}C_{H^s}C_{\rm P,\Omega}^{(1)}\|\underline{\rm curl}(\underline{\mathsf{L}}_{\mathcal{E}}^{\rm conf}(\mathbf{u}))\|_{L^2(\Omega)^3},$$

whence we infer (21) with $C_{\rm P}^{(1)}=\eta_\alpha^{-1}C_{\rm N}C_{H^s}C_{\rm P,\Omega}^{(1)}C_{\mathcal{F}}^{\sharp}$ observing that $\underline{\rm curl}(\underline{z})=\underline{\rm curl}(\underline{\mathsf{L}}_{\mathcal{E}}^{\rm conf}(\mathbf{u}))=\underline{\mathsf{L}}_{\mathcal{F}}^{\rm conf}(\mathsf{CURL}(\mathbf{u}))$ and using the stability of $\underline{\mathsf{L}}_{\mathcal{F}}^{\rm conf}$. □

References

[1] H. Abboud, F. E. Chami, and T. Sayah. A priori and a posteriori estimates for three-dimensional Stokes equations with nonstandard boundary conditions. *Numer. Methods Partial Differential Equations*, 28(4):1178–1193, 2012.

[2] C. Amrouche, C. Bernardi, M. Dauge, and V. Girault. Vector potentials in three-dimensional non-smooth domains. *Math. Meth. Appl. Sci.*, 21(9):823–864, 1998.

[3] B. Andreianov, M. Bendahmane, F. Hubert, and S. Krell. On 3D DDFV discretization of gradient and divergence operators. I. meshing, operators and discrete duality. *IMA Journal of Numerical Analysis*, 32(4):1574–1603, 2012.

[4] D. N. Arnold, R. S. Falk, and R. Winther. Finite Element Exterior Calculus: from Hodge Theory to Numerical Stability. *Bull. Amer. Math. Soc.*, 47:281–354, 2010. DOI: 10.1090/S0273-0979-10-01278-4.

[5] L. Beirão da Veiga, V. Gyrya, K. Lipnikov, and G. Manzini. Mimetic Finite Difference Method for the Stokes Problem on Polygonal Meshes. *Journal of Computational Physics*, 228(19):7215–7232, 2009.

[6] L. Beirão da Veiga, K. Lipnikov, and G. Manzini. Error analysis for mimetic discretization of the steady Stokes problem on polyhedral meshes. *SIAM J. Numer. Anal*, 48(4):1419–1443, 2010.

[7] C. Bernardi and N. Chorfi. Spectral discretization of the vorticity, velocity, and pressure formulation of the Stokes problem. *SIAM J. Numer. Anal*, 44:826–850, 2006.

[8] P. Bochev and J. M. Hyman. Principles of mimetic discretizations of differential operators. In D. Arnold, P. Bochev, R. Lehoucq, R. A. Nicolaides, and M. Shashkov, editors, *Compatible Spatial Discretization*, volume 142 of *The IMA Volumes in mathematics and its applications*, pages 89–120. Springer, 2005.

[9] J. Bonelle and A. Ern. Analysis of Compatible Discrete Operator Schemes for Elliptic Problems on Polyhedral Meshes. *ESAIM: Mathematical Modelling and Numerical Analysis*, 48(2):553–581, 2014. DOI:10.1051/m2an/2013104.

[10] A. Bossavit. Computational electromagnetism and geometry. *J. Japan Soc. Appl. Electromagn. & Mech.*, 7-8:150–9 (no 1), 294–301 (no 2), 401–8 (no 3), 102–9 (no 4), 203–9 (no 5), 372–7 (no 6), 1999-2000.

[11] J. H. Bramble and P. Lee. On Variational Formulations for the Stokes Equations with Non-Standard Boundary Conditions. *M2AN Math. Model. Numer. Anal.*, 28(7):903–919, 1994.

[12] F. Brezzi, A. Buffa, and K. Lipnikov. Mimetic Finite Difference for elliptic problem. *Mathematical Modelling and Numerical Analysis*, 43:277–295, 2009.

[13] F. Brezzi and M. Fortin. *Mixed and Hydbrid Finite Element Methods.* Springer series in computational mathematics. Springer-Verlag, 1991.

[14] F. Brezzi, K. Lipnikov, and M. Shashkov. Convergence of the Mimetic Finite Difference method for diffusion problems on polyhedral meshes. *SIAM J. Numer. Anal*, 43(5):1872–1896, 2005.

[15] S. H. Christiansen. A construction of spaces of compatible differential forms on cellular complexes. *Math. Models Methods Appl. Sci.*, 18(5):739–757, 2008.

[16] M. Clemens and T. Weiland. Discrete Electromagnetism with the Finite Integration Technique. *Progress In Electromagnetics Research*, 32:65–87, 2001.

[17] L. Codecasa, R. Specogna, and F. Trevisan. A new set of basis functions for the Discrete Geometric Approach. *Journal of Computational Physics*, 229(19):7401–7410, September 2010.

[18] L. Codecasa and F. Trevisan. Convergence of electromagnetic problems modelled by Discrete Geometric Approach. *CMES*, 58(1):pp. 15–44, 2010.

[19] S. Delcourte and P. Omnes. A Discrete Duality Finite Volume discretization of the vorticity-velocity-pressure formulation of the 2D Stokes problem on almost arbitrary two-dimensional grids. http://hal-cea.archives-ouvertes.fr/cea-00772972, 2013.

[20] M. Desbrun, A. N. Hirani, M. Leok, and J. E. Marsden. Discrete Exterior Calculus. http://arxiv.org/abs/math/0508341, 2005.

[21] D. A. Di Pietro and S. Lemaire. An extension of the Crouzeix-Raviart space to general meshes with application to quasi-incompressible linear elasticity and Stokes flow. *Math. Comp.*, 2014. Accepted for publication.

[22] J. Droniou and R. Eymard. A mixed finite volume scheme for anisotropic diffusion problems on any grid. *Numer. Math.*, 105(1):35–71, 2006.

[23] F. Dubois. Une formulation tourbillon-vitesse-presion pour le problème de Stokes. *Comptes Rendus de l'Académie des Sciences*, 314:277–280, 1992.

[24] F. Dubois. Vorticity-velocity-pressure formulation for the Stokes problem. *Mathematical Methods in the Applied Sciences*, 25(13):1091–1119, 2002.

[25] R. Eymard, J. Fuhrmann, and A. Linke. MAC schemes on triangular delaunay meshes. Technical Report 1654, WIAS, 2011.

[26] R. Eymard, G. Henry, R. Herbin, F. Hubert, R. Klöfkorn, and G. Manzini. 3D benchmark on discretization schemes for anisotropic diffusion problems on general grids. In *Finite Volumes for Complex Applications VI - Problems & Perspectives*, volume 2, pages 95–130. Springer, 2011.

[27] R. Falk and M. Neilan. Stokes Complexes and the Construction of Stable Finite Elements with Pointwise Mass Conservation. *SIAM J. Numer. Anal*, 51(2):1308–1326, 2013.

[28] M. Gerritsma. An introduction to a compatible spectral discretization method. *Mechanics of Advanced Materials and Structures*, 19(1-3):48–67, 2012.

[29] R. Hiptmair. Discrete Hodge operators: An algebraic perspective. *Progress In Electromagnetics Research*, 32:247–269, 2001.

[30] J. Kreeft and M. Gerritsma. Mixed mimetic spectral element method for Stokes flow: A pointwise divergence-free solution. *Journal of Computational Physics*, 240:284–309, 2013.

[31] S. Krell and G. Manzini. The Discrete Duality Finite Volume method for Stokes equations on three-dimensional polyhedral meshes. *SIAM Journal on Numerical Analysis*, 50, 2012.

[32] Alexander Linke. On the role of the Helmholtz decomposition in mixed methods for incompressible flows and a new variational crime. *Comput. Methods Appl. Mech. Engrg.*, 268:782–800, 2014.

[33] C. Mattiussi. The finite volume, finite element, and finite difference methods as numerical methods for physical field problems. *Advances in Imaging and electron physics*, 113:1–146, 2000.

[34] P. Monk. *Finite Element Methods for Maxwell's Equations*. Numerical Mathematics and Scientific Computation. The Clarendon Press Oxford University Press, 2003.

[35] J. C. Nédélec. Élements Finis Mixtes Incompressibles pour l'Équation de Stokes dans $\mathbb{R}^3$. *Numer. Math.*, 39:97–112, 1982.

[36] J. B. Perot. Discrete Conservation Properties of Unstructured Mesh Schemes. *Annual Review of Fluid Mechanics*, 43(1):299–318, 2011.

[37] J. B. Perot and R. Nallapati. A moving unstructured staggered mesh method for the simulation of incompressible free-surface flows. *Journal of Computational Physics*, 184(1):192–214, 2003.

[38] J. B. Perot and V. Subramanian. Discrete calculus methods for diffusion. *Journal of Computational Physics*, 224(1):59–81, 2007.

[39] T. Tarhasaari, L. Kettunen, and A. Bossavit. Some realizations of a discrete Hodge operator: A reinterpretation of finite element techniques. *IEEE Transactions on magnetics*, 35(3):1494–1497, 1999.

[40] F.L. Teixeira. Differential Forms in Lattice Field Theories: An Overview. *ISRN Mathematical Physics*, 2013:16p, 2013.

[41] E. Tonti. *On the formal structure of physical theories.* Istituto di matematica, Politecnico, Milano, 1975.

[42] E. Tonti. Finite formulation of the electromagnetic field. *Progress In Electromagnetics Research (PIER)*, 32:1–44, 2001.

[43] S. Zaglmayr. *High order finite element methods for electromagnetic field computation.* PhD thesis, Johannes Kepler Universität Linz, 2006.